

**TECHNICAL UNIVERSITY OF LIBEREC**  
**FACULTY OF TEXTILE ENGINEERING**



**DIPLOMA THESIS**

**By Mduduzi Blessing Khumalo**

**Year: 2012**

Technical University of Liberec  
Faculty of Textile Engineering  
Department of Textile Technology  
MSc Textile Engineering

**Diploma Thesis**

**Study of the Roller Electrospinning  
with Regard to Roller Movement**

By:  
**Mduduzi Blessing Kumalo**

Supervisor:  
**Professor Oldrich Jirsak**

### **Statement**

I have been informed that on my thesis is fully applicable the Act No. 121/2000 Coll. about copyright, especially §60 - school work.

I acknowledge that Technical University of Liberec (TUL) does not breach my copyright when using my thesis for internal need of TUL.

Shall I use my thesis or shall I award a licence for its utilisation I acknowledge that I am obliged to inform TUL about this fact, TUL has right to claim expenses incurred for this thesis up to amount of actual full expenses.

I have elaborate the thesis alone utilising listed and on basis of consultations with supervisor.

Date:

Signature:

## ACKNOWLEDGEMENTS

I would like to give my sincere gratitude to my supervisor Prof. Oldrich Jirsak for his guidance in structuring this work and for his encouraging advises, and for all the support he gave me whatsoever. I would also like to thank my co-supervisor Miss Fatma Yener and Mr Baturalp Yalçinkaya for their dedicated support they gave me during my experiments. And I appreciate everyone in Technical university of Liberec who made this work successful.

My thanks also travel with the speed of light to Khumalo family back home in South Africa who was continuously sending love to me throughout my stay in Czech Republic. Lastly, but not least, thanks to my friends for all kind of support they gave me, “ngithi nje ningadinwa nangomuso”.

## ABSTRACT

The objective was to control the thickness of the layer of the polymer solution onto a spinning roller. Therefore, the effect of the angular speed of the spinning roller and viscosity of the polyvinyl alcohol solution on the thickness of the layer of the polymer solution onto a spinning roller was investigated. The concentration of the solution was kept constant while changing roller angular speed; accordingly, the roller angular speed was kept constant while varying concentration and the thickness of the layer of the polymer solution was measured, respectively. Sodium chloride was added into the solution to change viscosity of the solution.

The effects of roller speed and viscosity were visually observed onto the roller surface by video camera, analyzing the number of Taylor cones. Current test was also used to analyze the spinning progress. The properties of materials, such as spinning performance and fiber diameters were analyzed.

It has been concluded that the thickness of the solution layer increases when the viscosity (as a function of concentration) of the solution increases. It has been also proven that the increase in the angular speed of the spinning roller causes an increase in the thickness of the solution layer onto the roller. Throughput of the product and diameters of nanofibers are both directly proportional to angular speed of the roller and viscosity of the solution. Therefore, the thicker is the layer of the polymer solution on top of the spinning roller the improved are fabric throughput and nanofiber diameter. These work proved that adding sodium chloride into polyvinyl alcohol to change its viscosity, affect, inversely, the electrospinning progress, fabric throughput and nanofibers diameters.

Finally, the researcher adds roller movement and solution rheology into the family of parameters of roller electrospinning, since it affect both the spinning progress and produced material.

## Table of Contents

Chapter 1 : Electrospinning .....	12
1.1 History .....	12
1.2 Potential applications.....	14
1.3 Fundamental of Electrospinning.....	15
1.3.1 Needle Electrospinning.....	15
1.3.2 Needleless (Roller) Electrospinning.....	16
1.4 Objective of the work .....	18
Chapter 2 : Roller and rheology.....	19
2.1 Roller movement in roller electrospinning.....	19
2.1.1 Viscosity of the polymer solution.....	21
2.2 Summary of theoretical study and the aim of the work.....	23
Chapter 3 : Parameters of roller electrospinning.....	24
3.1 Independent parameters of roller electrospinning .....	24
3.1.1 Solution properties.....	24
3.1.1.1 Viscosity of the polymer solution.....	24
3.1.1.2 Surface Tension .....	25
3.1.1.3 Conductivity/surface charge density.....	25
3.1.2 Process parameters of roller electrospinning.....	26
3.1.2.1 Applied voltage.....	26
3.1.2.2 Type of collector [3] .....	27
3.1.2.3 Velocity of the collector .....	27
3.1.2.4 Roller to collector distance .....	27
3.1.2.5 Speed of rotation of roller.....	28
3.1.2.6 Ambient parameters.....	28
3.2 Dependent parameters of roller electrospinning [3] .....	28
3.2.1 Density of Taylor cones (D) .....	28
3.2.2 Life time of jet .....	29
3.2.4 Spinning performance (SP) [3].....	29
3.2.5 Spinning performance per cone .....	30
3.2.6 Non-fibrous area (NFA) .....	30
3.2.7 Fibers diameter .....	30
3.2.8 Fibers diameter distribution.....	31

Chapter 4 : Experimental .....	32
4.1 Experiments performed .....	32
4.1.2 Roller electrospinning.....	32
4.2 Material.....	32
4.3 Method.....	33
4.3.1 Film thickness measurement.....	33
4.3.2 Roller electrospinning.....	34
Chapter 5 : Results and discussions.....	36
5.1 Viscosity, conductivity and surface tension .....	36
Discussion of section 5.1 .....	38
5.2 Thickness of the layer of PVA solution on the roller .....	38
Discussion of section 5.2 .....	41
5.3 Roller Electrospinning .....	41
5.3.1 Effect of concentration on roller electrospinning .....	41
Discussion of section 5.3.1 .....	47
5.3.2 Effect of roller speed on roller electrospinning .....	47
Discussion of section 5.3.2 .....	53
5.3.3 Effect of sodium salt on roller electrospinning.....	53
Discussion of section 5.3.3 .....	59
Chapter 6 : Conclusion .....	60
References .....	61

## List of symbols

$\Theta$	azimuthal direction, rad
$\mu$	Viscosity, Pa s
$\rho$	density, kg.m <sup>-3</sup>
$\phi$	$\theta/K$
$\omega$	angular speed of roller, rad s <sup>-1</sup>

## List of abbreviations

F	force, N
Q	charge, C
r	radius, m
d	diameter, m
l	length, in m
E	electric fields strength, N/C
G	gravitational acceleration $9.8 \text{ m/s}^{-2}$
h	film thickness, m
$h^*$	$(\mu^* / \rho g)^{1/2}$ , characteristic thickness, m
H	$h/h^*$ , dimensionless thickness
SP	Spinning performance, in g/m/min
G	weight of nanofibers membrane per area in $\text{g/m}^2$
n	number of elements [-]

## List of figures

Figure 1.1:	Schematic diagram of needle electrospinning.....	15
Figure 1.2:	Schematic diagram of needleless (roller) Electrospinning.....	16
Figure 2.1:	Overall system geometry.....	19
Figure 2.2:	Graph of dimensionless thickness (H) as a function of immersion angle $\phi$ .....	20
Figure 2.3:	A volume of liquid subjected to an applied shear stress.....	22
Figure 2.4:	Dependence of viscosity on the shear rate for a Newtonian liquid and a non-Newtonian pseudoplastic polymer solution.....	22
Figure 3.1:	Non-fibrous areas.....	30
Figure 4.1:	Cylinder (diameter of 20 mm) immersed into the polymer solution.....	33
Figure 4.2:	Schematic diagram of roller electrospinning set up.....	34
Figure 5.1:	Graph of zero shear viscosity as a function of concentration (%)......	36
Figure 5.2:	Graph of conductivity (mS/cm) at different PVA concentration (%)......	37
Figure 5.3:	Graph of conductivity (mS/cm) of 12% PVA with various NaCl (%)......	37
Figure 5.4:	Graph of thickness (mm) of the layer of PVA solutions (with different concentrations) on the roller surface as the function roller's rotation (rpm).....	39
Figure 5.5:	The graph shows the effect of PVA concentration (%) on the thickness of the layer (mm) of the PVA solution onto the spinning roller.....	39
Figure 5.6:	The graphs of thickness (mm) of the layer of PVA solutions as the function viscosity (Pa.s) at indicated roller speeds.....	40
Figure 5.7:	Graph of thickness (mm) of the layer of PVA solutions (with different NaCl concentrations) on the surface of the roller at different roller speed (rpm).....	40



Figure 5.8: Graph of electrical current ( $\mu\text{A}$ ) in electrospinning of 7% PVA solution versus time (s).....	42
Figure 5.9: Graph of electrical current ( $\mu\text{A}$ ) in spinning of 9% PVA solution versus time (s).....	42
Figure 5.10: Graph of electrical current ( $\mu\text{A}$ ) in electrospinning of 12% PVA solution versus time (s).....	43
Figure 5.11: Graph of electrical current ( $\mu\text{A}$ ) flowing through the system during electrospinning of 15% PVA solution versus time (s). ....	43
Figure 5.12: Graph of spinning performance SP (g/min/m) as a function PVA concentration (%).....	44
Figure 5.13: Graph of flowing current ( $\mu\text{A}$ ) in the spinning system versus PVA concentration (%).....	45
Figure 5.14: Graphs show the dependence of number of Taylor cones and throughput SP per jet (mg/min) on the PVA concentration (%). ....	45
Figure 5.15: Graphs show the dependence of current ( $\mu\text{A}$ ) and throughput SP per jet (g/min) on the PVA concentration (%). ....	46
Figure 5.16: The graph of nanofiber (nm) diameters vs concentration of polyvinyl alcohol (%).....	46
Figure 5.17: Graph of the current ( $\mu\text{A}$ ) flowing through the system in electrospinning of 12% PVA solution versus time (s) while roller speed was 1.5 rpm. ....	48
Figure 5.18: Graph of the current ( $\mu\text{A}$ ) flowing through the system in electrospinning of 12% PVA solution versus time (s).....	48
Figure 5.19: Graph of the current ( $\mu\text{A}$ ) flowing through the system in electrospinning of 12% PVA solution versus time (s) while roller speed was 3 rpm. ....	49
Figure 5.20: Graph of the current ( $\mu\text{A}$ ) flowing through the system in electrospinning of 12%PVA solution versus time (s) while roller speed was 4 rpm. ....	49
Figure 5.21: Graph of the current ( $\mu\text{A}$ ) flowing through the system in electrospinning of 12% PVA solution versus time (s) while roller speed was 5 rpm. ....	50
Figure 5.22: Graph of spinning performance or throughput SP (g/min/m) versus roller speed (rpm).....	51
Figure 5.23: The graph shows the dependence of number of Taylor cones and electrical current on roller speed. ....	51
Figure 5.24: The graph shows the effect of roller speed on current per jet ( $\mu\text{A}$ ) and throughput per jet SP/jet (g/min).....	52
Figure 5.25: The graph of nanofibers diameters (nm) as a function of roller speed (rpm).....	52
Figure 5.26: Graph of electrical current ( $\mu\text{A}$ ) in electrospinning of 12% PVA solution without NaCl versus time (s). ....	53
Figure 5.27: Graph of electrical current ( $\mu\text{A}$ ) flowing through the system during electrospinning of 12% PVA with 0.1%NaCl solution versus time (s). ....	54

Figure 5.28: Graph of electrical current ( $\mu\text{A}$ ) flowing through the system during electrospinning of 12% PVA with 0.2%NaCl solution versus time (s). .....	54
Figure 5.29: Graph of electrical current ( $\mu\text{A}$ ) flowing through the system during electrospinning of 12% PVA with 0.5%NaCl solution versus time (s). .....	55
Figure 5.30: Graph of electrical current ( $\mu\text{A}$ ) flowing through the system during electrospinning of 12% PVA with 1%NaCl solution versus time (s). .....	55
Figure 5.31: Graph shows the starting time (s) of cone formation versus sodium chloride, NaCl concentration (%). .....	56
Figure 5.32: Graph of spinning performance SP (g/min/m) versus sodium chloride NaCl concentration (%). .....	57
Figure 5.33: Graph of current ( $\mu\text{A}$ ) flowing through the spinning system versus sodium chloride concentration (%) in a polyvinyl alcohol solution. ....	57
Figure 5.34: Graph shows the dependence of number of Taylor cones and current per jet on sodium chloride concentration. ....	58
Figure 5.35: Graph shows the dependence of spinning performance per jet (mg/min) and current ( $\mu\text{A}$ ) per jet on sodium chloride concentration. ....	58
Figure 5.36: Graph of fiber diameters (nm) as function of concentration (%) of sodium chloride in polyvinyl alcohol solution. ....	59

## List of Tables

Table 4.1:	Prepared solutions for experiment.....	33
Table 4.2:	Spinning conditions.....	34
Table 5.1:	Viscosity, surface tension and conductivity of different PVA solutions.....	36
Table 5.2:	Thickness of the layer (mm) of PVA solution as the function of roller speed. ....	38
Table 5.3:	The table of PVA concentration-dependent parameters in electrospinning. ....	44
Table 5.4:	The table tabulates the parameters of electrospinning for the investigation of the effect of roller speed (rpm).....	47
Table 5.5:	The table contains parameters that depend on roller speed for electrospinning of 12% PVA solution.....	50
Table 5.6:	The table contains dependent parameters in different sodium chloride concentration. ....	56

## Chapter 1 : Electrospinning

The discovery of the formation of nanofibers from polymer solution using electrostatic forces seemed to be a major finding, but that was just the beginning of the series of researches carried out to understand the whole mechanism of electrospinning. Nanofiber's electrospinning is still under research departments even though it was found decades ago, there are number of publications done to have better understanding of this method.

Unlike conventional fiber spinning techniques (wet spinning, dry spinning, melt spinning, gel spinning), which are capable of producing polymer fibers with diameters down to the micrometer range, electrostatic spinning, or 'electrospinning' is a process capable of producing polymer fibers in the nanometer diameter range. Electrospinning is a novel and efficient fabrication process that can be utilized to assemble fibrous polymer mats composed of fiber diameters ranging from several microns down to fibers with diameter lower than 100 nm [1].

Up to so far; there are only two types of electrospinning, needle and needleless electrospinning. Needle electrospinning was the first technology for electrospinning of nanofibers to be discovered, and it has been studied thoroughly from the mechanism of the technology to the properties of its nanofibers.

However, the foresee limitations of needle electrospinning (commercially) had led to its replacement by nanospider technology. The invention was based on the realization that the needle electrospinning can be replaced by a much more productive process that would be suitable for industrial application [2]. This equipment, which is first patented by Jirsak, enables to produce membranes collected fibers in a range from 100 to 600 nm of diameter [3].

### 1.1 History

Electrospinning followed the William Gibert's findings of the behavior of an electrically charged water droplet. In the late 15th century William Gilbert set out to describe the behavior of magnetic and electrostatic phenomena. He observed that when a suitably electrically charged piece of amber was brought near a droplet of water it would form a cone shape and small droplets would be ejected from the tip of the cone: this is the first recorded observation of electrospaying.

In 1902 Cooley J.F described in his patent (United State 692631) a process of using high voltage power supplies to generate yarn. Even at this early stage it was recognized that to form fibers rather than droplets the fluid must be sufficiently viscous, solvent volatile enough to evaporate to allow regeneration of the solid polymer, and electric field strength within a certain range.

For further analysis, Zeleny J published work in 1914, on the behavior of fluid droplets at the end of metal capillaries. His effort began the attempt to mathematically model the behavior of fluids under electrostatic forces. The method of electrodynamic atomization of liquids in which a slightly-conducting-liquid discharged from metering nozzle subjected to a

high DC potential difference is atomized by forces of repulsion of similarly charged electric charges into very fine particles which can then be precipitated onto an oppositely charged electrode, is the original of process of electro spinning of fibrous materials.

Bose found, at the very first attempt of investigating this phenomena in 1745 that, under certain conditions, the clouds of atomized droplets is preceded by a jet flow [3]. Further developments toward commercialization were made by Anton Formhals, and described in a sequence of patents from 1934 entitled "Process and Apparatus for Preparing Artificial Threads" (United State Patent 1,975,504) to "Method and Apparatus for Spinning" (United State Patent 2,349,950) published in 1944 for the fabrication of textile yarns.

In 1938, N.D. Rozenblum and I.V. Petryanov-Sokolov, working with Prof. N.A. Fuks in the USSR, generated electrospun fibers, which they developed into filter materials known as "Petryanov filters". The experiment was conducted using cellulose acetate solution atomized by the method of electrodynamic, in which the liquid discharged from the nozzle subjected to high potential difference, and solidified completely, forming fibers having micron-scale diameters or even smaller than that. Begell House Inc. published the book called "Electrospinning of Micro- and Nanofibers: Fundamentals in Separation and Filtration Processes" which is based on the work that was done by Rozenblum N.D. and Petryanov-Sokolov I.V. The book explain mechanism of electrospinning of fibrous materials and the structure of these materials, raw materials, effect of the properties of the spinning solution on the course of formation and properties of fibers, technology of electrospinning of fibrous materials (Petryanov Filters), etc.

Between 1964 and 1969 Sir Geoffrey Ingram Taylor contributed to electrospinning by mathematically modeling the shape of the cone formed by the fluid droplet under the effect of an electric field; this characteristic droplet shape is now known as the Taylor cone. He theoretically derived based on general assumptions that the requirements to form a perfect cone under electrospinning conditions required a semi-vertical angle of  $49.3^\circ$  (a whole angle of  $98.6^\circ$ ) and demonstrated that the shape of such a cone approached the theoretical shape just before jet formation. Taylor's derivation is based on two assumptions: (1) that the surface of the cone is an equipotential surface and (2) that the cone exists in steady state equilibrium. To meet both of these criteria the electric field must have azimuthal symmetry and have square of the radius dependence to counter the surface tension to produce the cone.

In the early 1990s several research groups (notably that of Reneker and Rutledge who popularized the name electrospinning for the process) demonstrated that many organic polymers could be electrospun into nanofibers. Since then, the number of publications about electrospinning has been increasing exponentially every year. Since 1995 there have been further theoretical developments of the driving mechanisms of the electrospinning process. Reznik describes extensive work on the shape of the Taylor cone and the subsequent ejection of a fluid jet.

Work by Hohman investigates the relative growth rates of the numerous proposed instabilities in an electrically forced jet once in flight and endeavors to describe the most important instability to the electrospinning process, the bending instability.

The researches have been continuing ever since, but all were focused to needle electrospinning. Nanospider technology was introduced as the unique commercial equipment to produce nanofibers-web via needleless electrospinning technology. This equipment is first patented by Jirsak .O from Technical university of Liberec, and then it is developed by Czech company Elmarco, Liberec to enables to use in industrial production of non-woven textiles.

This equipment can produce membranes collected fibers in a range from 100 to 600 nm of diameter. Such materials are widely utilized in many fields, as filtration, healthcare, building construction, automotive industry, cosmetics and many others. Elmarco produced the pilot manufacturing line for nanofiber production in 2004, and in 2006 offered the first models for industrial production. Recent models of Nanospiders have production rate up to 30 m/min with the fabric width bigger than 1 m [3].

## 1.2 Potential applications

The enthusiasm of all these researchers to research about electrospinning of nanofibers is driven by the foreknown potential applications. The abilities of the researchers to controller the fiber morphology, fiber diameter and fiber installation provide the insight of the nanofibers possible application. The most of them will change lives of many soul holders, and even save lives of others because there is space for nanofibers in medical industry. The properties of nanofibers, such as low pressure drop, large surface area, etc. are the reasons of the following predicted uses:

- Applications in life science
  - ⊗ Drug delivery carrier
  - ⊗ Affinity membrane
  - ⊗ Wound dressing
  
- Tissue engineering scaffolding
  - ⊗ Porous membrane for skin
  - ⊗ Tubular shapes for blood vessels and nerve regenerations
  - ⊗ Three dimensions scaffold for bone and cartilage regenerations
  
- Military protecting clothing
  - ⊗ Minimal impedance to air
  - ⊗ Efficiency in trapping aerosol particles
  - ⊗ Anti-biochemical gases
  
- Filters
  - ⊗ Liquid filtration
  - ⊗ Gas filtration
  - ⊗ Molecule filtration

- Cosmetic skin mask
  - ⊗ Skin cleaning
  - ⊗ Skin healing
  - ⊗ Skin therapy with medicine
  
- Nano sensors
  - ⊗ Thermal sensors
  - ⊗ Electric sensors
  - ⊗ Biochemical sensors
  - ⊗ Fluorescence optical chemical sensors
  
- Energy conversion and storage
  - ⊗ Batteries
  - ⊗ Photovoltaic cell
  - ⊗ Hydrogen-storage
  
- Other industrial applications include:
  - ⊗ Reinforcement
  - ⊗ And Sound absorption.

### 1.3 Fundamental of Electrospinning

In electrospinning, a high voltage is applied to a polymer fluid such that charges are induced within the fluid. When charges within the fluid reached a critical amount, a fluid jet will erupt from the droplet resulting in the formation of a Taylor cone. The electrospinning jet will travel towards the region of lower potential, which in most cases, is a grounded collector [4]. As it has been mentioned before, there are only two electrospinning technologies up to now, needle and needleless electrospinning.

#### 1.3.1 Needle Electrospinning

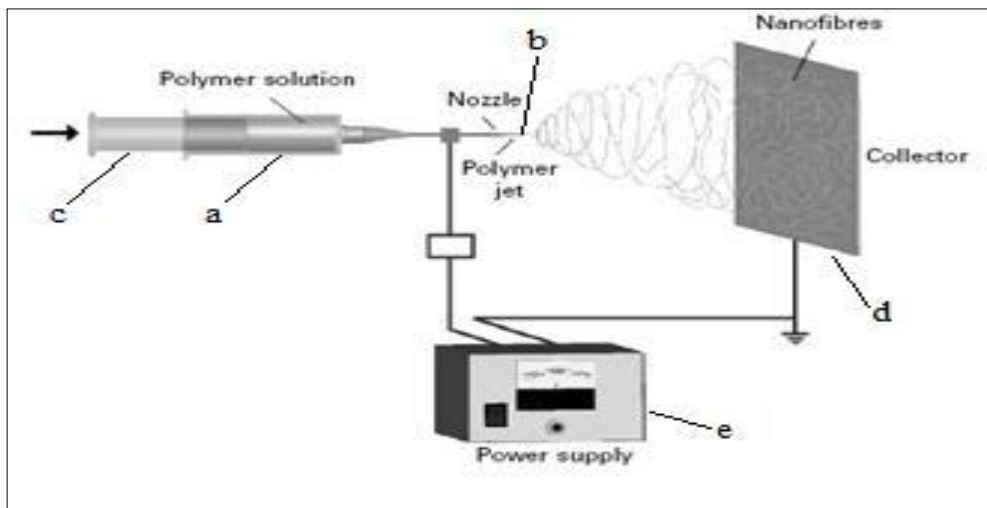


**Figure 1.1:** Schematic diagram of needle electrospinning.

Figure 1.1 shows the schematic diagram of the needle electrospinning. It consists of a syringe (a), hollow needle (b), feeding mechanism (c), a grounded collector electrode (d) and a source of high voltage (e). The high voltage connected to the hollow needle, charge the polymer solution. Taylor cone is formed at the tip of hollow needle owing to the electric fields. A polymer jet moves out of the tip of Taylor cone which is subsequently converted into submicron fibers [3].

### 1.3.2 Needleless (Roller) Electrospinning

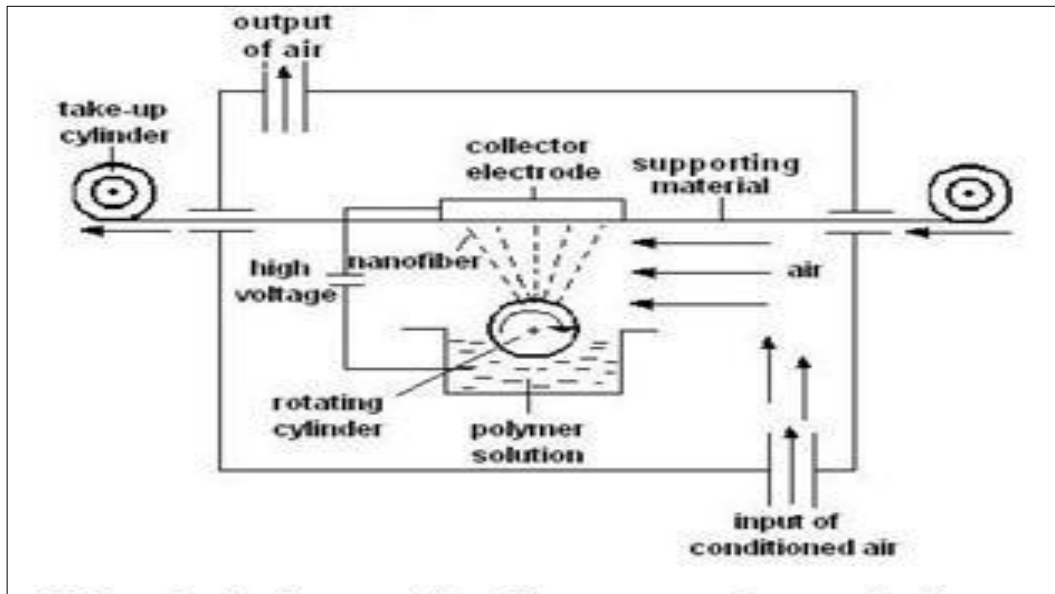


**Figure 1.2:** Schematic diagram of needleless (roller) Electrospinning.

The roller is fairly immersed into the polymer solution. High voltage is connected to the roller, then the roller slowly rotate, picking up the polymer solution onto its surface. Charged polymer solution form many Taylor cones on the surface of the roller, and produce the nanofibers. On the opposite side of the formed nanofibers is collector which is normally grounded. The high potential difference between the roller and the collector allows easy transportation of nanofibers from roller to the collector by electric fields. The transportation success is due to the Coulomb's law which describes the force between two point charges, for electrospinning, point charges can be related to charged polymer solution and charged collector. It states that the magnitude of the electrostatic force  $F(N)$  between two point charges  $Q_1 (C)$  and  $Q_2 (C)$  is directly proportional to the product of the magnitudes of each charge and inversely proportional to the square of the distance  $r(m)$  between them:

$$F = \frac{Q_1 Q_2}{4\pi r^2 \epsilon_0} \quad (1.1)$$



Whereas  $r$  in m is the distance between two point charges, Taylor cone and collector, while  $Q_1$  and  $Q_2$  in C represent the charges of Taylor cone and collector, respectively.  $\epsilon_0$  is a constant called the permittivity of free space. However, this law is only valid if the charges involved are point charges. In most practical cases, the electric field is more widely used and it is defined as a region where a charge (polymer) feels a force created by other charges (collector). The magnitude of the electric force experienced by point charge (polymer solution) due to field strength is as follows.

$$F = qE \quad (1.2)$$

where  $F$  (N) is the force  $q$ (C) is the charge  $E$  (N/C) is the electric field strength. For a positive charge, the force has the same direction as the field strength while a negative charge will have the force at the opposite direction. Given a charge  $q$ , the field strength at a distance  $d$  is written as,

$$E = \frac{q}{4\pi\epsilon d^2} \quad (1.3)$$

Eq.1.3 is the relevant description for the transportation of nanofibers to the collector. Flying polymer jets may be expected to entangle themselves along the way to the collector, but the repulsive forces (since like charges repel) between jets keep them apart from each other. Intermolecular force of attraction in between the liquid units maintains them together in a polymer jet.

Tuan D. A, in his work “the role of rheological properties of polymer solutions in needleless electrostatic spinning” [3] describes electrospinning as the process of three stages.

In the first stage, the polymer solution is carried onto the roller surface due to roller rotation. The high electric potential applied in the solution leads to the formation of Taylor cones, and then jets are produced. In the presence of electric fields, the jets are discharged from roller's surface. The shortening of the distance between jets and collector causes the jets to steadily accelerate, as shown in [eq.1.3] and thin out along an axis aligned with the general direction of electric field. This is an important stage because the stability and results of it controls all its subsequent stages and, in the final analysis, the desired properties of the finished fiber.

The second stage consists of several simultaneously occurring processes. In it, the fluctuations of the electric lines of force, caused by time and space variation of the bulk density of electrical charges, causes jets to turn transversely to the field direction and to be decelerated by the constantly increasing drag force of the gas. This produces a cloud that expands toward the collector by action of same polarity charges. At the same time, the rate of vaporization of the solvent that started already at the first stage of the process is steeply intensified, the jet solidifies and the resulting fibrous cloud drifts in the applied electric field onto collector. At this stage the jet may still undergo a sequence of splitting resulting in the formation of an unsteady bulk fiber-mesh structure.

The following, third stage also consists of two simultaneous processes: the first consisting of random deposition of fibers into a layer on collector and the second of a gas spark discharge between collector and the fiber layer forming on it, that closes the electric circuit.

## **1.4 Objective of the work**

Even though most of the parameters of roller electrospinning have been considered in the needle electrospinning, there are those that are completely new in electrospinning. The focal point of the author in this work is to study the effects of the thickness of the layer of polymer solution on top of the roller surface on roller electrospinning. Roller angular speed and viscosity of the polymer solution will be used control the thickness of the layer of polymer solution onto the roller surface. This investigation is important for controlling the production of nanofibers and their morphology. After the thickness of the layer of the polymer solution analysis, the effect of layer thickness to electrospinning (Taylor cone formation, polymer jet, material throughput and nanofiber diameters) will be analyzed. Furthermore, the question of how the addition of salt in polymer solution is affecting the roller electrospinning will be investigated.

## Chapter 2 : Roller and rheology

### 2.1 Roller movement in roller electrospinning

In order for roller electrospinning to start successfully, it is important that the roller immersed in a polymer solution, rotate to bring the polymer solution on its surface. It is necessary to examine this movement (rotation) since it determines the amount of polymer solution on the surface, and, the amount of solution together with voltage on the surface determine the input material of Taylor cone. The effect of roller rotation on the thickness of the layer of the polymer solution has been examined in different focuses. Campanella and Cerro [55] mathematically analyzed the viscous flow on a horizontal rotating cylinder. Figure 2.1 below shows the geometry of their system. A cylinder of radius  $R$  and infinite length was partially submerged in a pool of viscous fluid. The density  $\rho$ , viscosity  $\mu$  and surface tension  $\sigma$  of the fluid were known. Also known was immersion angle  $\theta_0$ , which described the flooding of the cylinder. The cylinder was rotating around its own axis at an angular speed  $\omega$ .

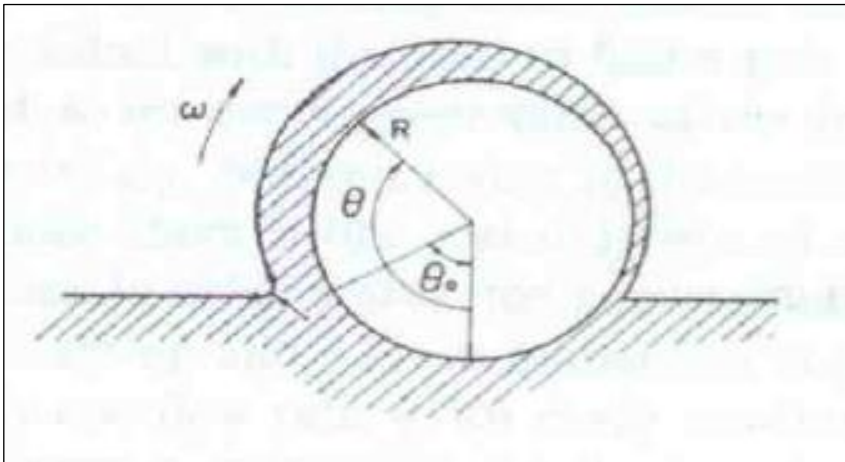


**Figure 2.1:** Overall system geometry [55].

Campanella and Cerro used the rapid flow approximation done by Cerro and Scriven [57] to simplify the equation of motion in order to a relationship between film thickness and operating parameters.

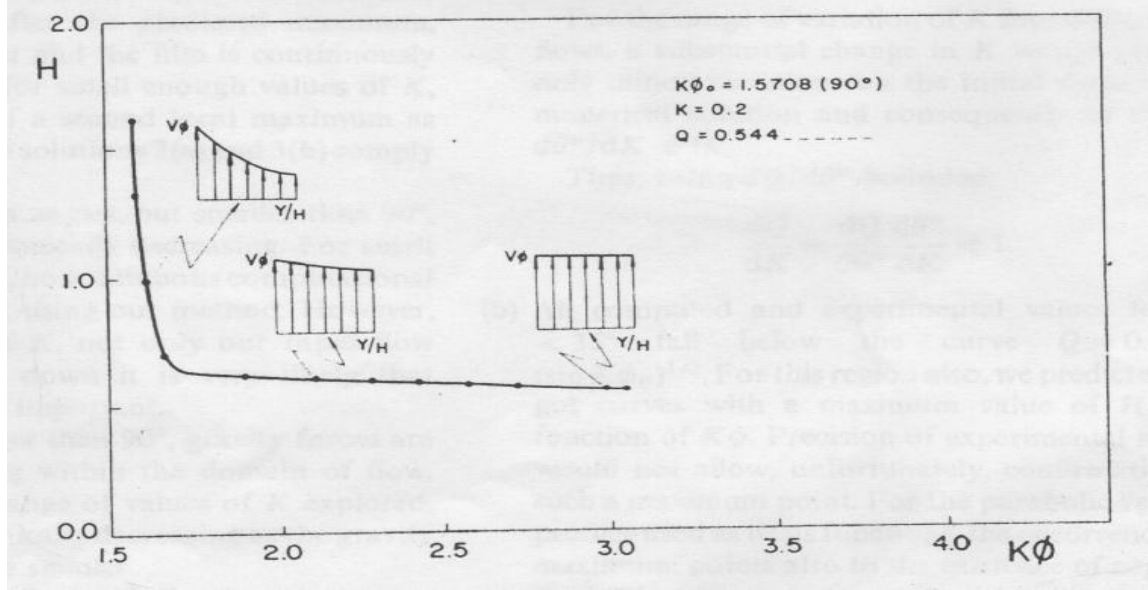


**Figure 2.2:** Graph of dimensionless thickness ( $H$ ) as a function of immersion angle  $\phi$  [55].

Keeping in mind the fact that gravity forces in the longitudinal direction of flow (i.e. azimuthally) are minimal at the lower part of the cylinder and grow to a maximum for  $\theta_0 = 90^\circ$ . Depending on the angle of immersion, the flow will be subject to a growing ( $K\phi_0 < 90^\circ$ ) or diminishing ( $K\phi_0 > 90^\circ$ ) force of gravity. For small immersion angles gravity increases as the film moves upwards causing a maximum film thickness as shown in Figure.2.2. After the predicted maximum, viscous forces take over and the film is continuously accelerated, hence, the solution layer becomes thinner.

Figure 2.2 shows the decrease in dimensionless thickness  $H$  [-] as the product  $K\phi$  increases, while  $H$ ,  $K$  and  $\phi$  are defined as follows:

$$H(\phi) = \frac{h}{h^*}, \quad h^* = \sqrt{\frac{uu^*}{\rho g}} \quad (2.1)$$

$$\theta = K\phi, \quad K = \frac{u^{*2}}{Rg} \quad (2.2)$$

Equation 2.1 shows that the increase in speed rotation of the roller and viscosity of the fluid lead to higher thickness of the fluid of on the surface of the roller. And equation 2.2 in simplicity state that the deeper is the roller on the fluid the thicker is the layer on the surface. Benjamin [56] in his work in (1995) also concluded that the amount of raised fluid by roller is a function of roller speed, immersion depth and rheological and interfacial properties of fluid. If the roller is deepen into the feeding pan, and then the thickness of the film onto the roller can be estimated with the result from deep coating theory as follows:

$$h = 0.994 \left[ \frac{\mu V}{\sigma} \right]^{1/6} \left[ \frac{\mu V}{\rho g (1 - \sin \theta)} \right]^{1/2} \quad (2.3)$$

provided that  $\mu V / \sigma < 10^{-2}$ . The film thickness is a function of the absolute speed of roller,  $V$ , gravity,  $g$ , the angle of inclination of the roller as it leaves the liquid,  $\theta$ , and the physical properties of the liquid:  $\sigma$  is the surface tension,  $\mu$  is the viscosity,  $\rho$  is the density.

Most of the investigations show that the thickness of the layer of the polymer solution on the roller surface depends, firstly, on the viscosity of polymer solution, which is the function of solution concentration and molecular weight, high viscous solution forms thicker layer. Secondly, the thickness is a function of roller movement (rotation), the faster is the roller, and the thicker is the solution layer on the roller surface. However, high speed allows air into the liquid and also allows splashing and mixing in the pan. Therefore, it is a wise idea to look closer to solution viscosity and roller speed in order to control them in roller electrospinning process.

### 2.1.1 Viscosity of the polymer solution

As mentioned in section 2.1.1, the viscosity of the solution in roller electrospinning plays an important role in bringing the polymer solution on the surface of the roller. It is very important in roller electrospinning to have enough polymer solution on the roller surface since this is where the Taylor cones are formed, therefore viscosity is necessary for successful start of roller electrospinning. It has been seen in equation 2.2 in Campanella and Cerro [55] work that polymer layer thickness is directly proportional to the square root of viscosity. And equation 2.3 in Benjamin [56] in his work in (1995) also conclude that thickness of the layer of the solution on the roller is directly proportional to viscosity to the power one in twelve; hence, increasing viscosity will indeed increase the thickness of polymer solution layer on the roller surface. However, there is an upper limit for viscosity in roller electrospinning. High viscosity resists the elongation of jet which results in nonofibers having large diameter. High viscosity also discourages the bending instability to set in for a longer distance as it emerges from the roller surface. As a result, the jet path is reduced and the bending instability spreads over a smaller area [Mituppatham et. al. (2004)].

The basic notion of solution viscosity is illustrated in Fig.2.1 of a volume of fluid in a shear field

(for instance a film of polymer solution confined between parallel plates where one is stationary and the other is moving in the  $x$ -direction at a constant velocity  $v$ . Assuming no slippage between the liquid and the plate, the force  $F$  per unit area  $A$  applied on the volume, the shear stress  $\tau$  results in a rate of deformation or a strain rate  $\dot{\gamma}$  where,

$$\tau = F / A, \quad \gamma = dv / dy, \quad \dot{\gamma} = d\gamma / dt = dv / dy. \quad (2.4)$$

The viscosity  $\eta$  of the fluid and the quantities  $\tau$  and  $\dot{\gamma}$  are related as follows:

$$\tau = \eta \dot{\gamma} \quad (2.5)$$

Where  $\eta$  is expressed in poise (P) = g/(cm.s) or Pas.

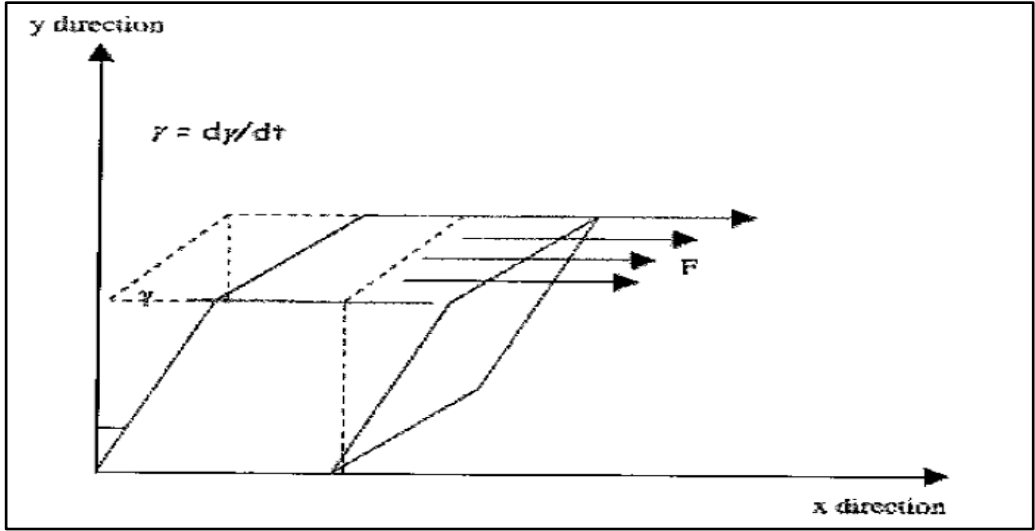


**Figure 2.3:** A volume of liquid subjected to an applied shear stress.

For simple low-molecular weight liquids, viscosity  $\eta$  is usually independent of the shear rate (i.e., the linear equation applies at constant temperature). Polymer solutions generally do not fall into this category of Newtonian liquids. At moderate shear rates polymer solutions generally show reduced viscosity or undergo shear-thinning. Fig.2.2 compares the shear rate dependence of viscosity for a Newtonian liquid and a non-Newtonian polymer solution. At very high shear rates, however, a non-Newtonian liquid may revert to Newtonian behavior.

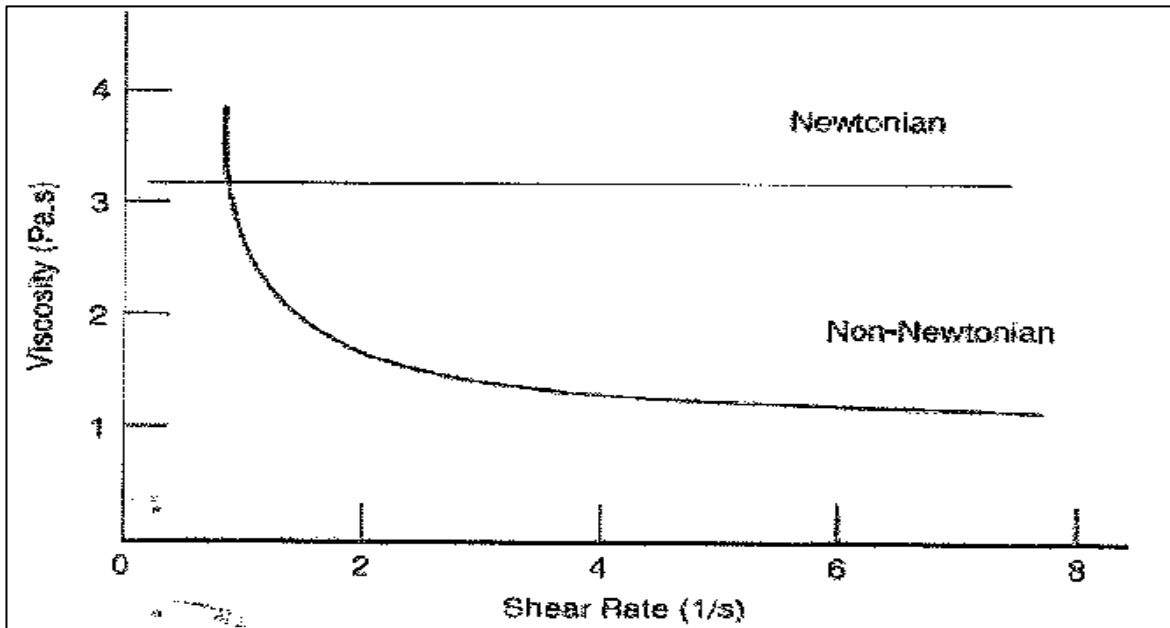


**Figure 2.4:** Dependence of viscosity on the shear rate for a Newtonian liquid and a non-Newtonian pseudoplastic polymer solution.

The viscosity  $\eta$  of a polymer solution (at a concentration  $c$ ) in a solvent viscosity  $\eta_{solv}$  is conveniently expressed by its relative  $\eta_r$ , and several other common measures:

$$\eta_r = \frac{\eta}{\eta_{solv}}, \quad \eta_{sp} = \frac{\eta - \eta_{solv}}{\eta_{solv}}, \quad \eta_{red} = \frac{1}{c} \left( \frac{\eta}{\eta_{solv}} - 1 \right) \quad (2.6)$$

Inherent viscosity

intrinsic viscosity

$$\eta = \frac{1}{c} \ln \eta_r \quad [\eta] = \lim_{c \rightarrow 0} \left( \frac{\eta_{sp}}{c} \right) \quad (2.7)$$

## 2.2 Summary of theoretical study and the aim of the work

Even if there are not much of publications about the thickness of the layer of the polymer solution on the surface of the roller in electrospinning, most of the related works such as pick-up roller in coating technology show that viscosity out of all other rheological properties of the solution is the most important parameter in roller electrospinning. It has been theoretically explained in section 2.3 that the increase in viscosity brings more polymer solution on top of the roller. As for the roller itself, it has to rotate in order to bring the solution in a spinnable position, therefore; it has been theoretically that increasing the roller rotation per minute results in more solution being brought on top of the roller surface.

**The main aims of this work are as follows:**

- To study the effect of solution concentration (viscosity) on the thickness of the layer of the of the polymer solution onto the rotating roller.
- To study the effect of roller rotational speed (in rpm) on the thickness of the polymer solution onto the roller.
- To investigate the effect of sodium chloride salt on the properties of the polymer (PVA) solution, and continue observe the effect on the roller electrospinning.

For complete understanding of these factors, the effects will be directly observed by counting Taylor cones on the roller, and the indirect method will be also used, where by independent parameters such as material throughput and fiber diameter will be analyzed. In addition, the effect of sodium chloride salt in roller electrospinning will be investigated.

## Chapter 3 : Parameters of roller electrospinning

This work of roller movement in roller electrospinning will form, if it is successful, the part of the parameters of roller electrospinning, which are divided into independent and dependent categories. The roller movement is considered to be part of independent parameters of roller electrospinning. The other parameters for roller electrospinning are shortly described below.

### 3.1 Independent parameters of roller electrospinning

Many parameters can influence the transformation of polymer solutions into nanofibers through electrospinning. These parameters include (a) the solution properties such as viscosity, conductivity and surface tension, (b) governing variables such as electric potential at the surface of the roller, and the distance between the surface of the roller and the collecting screen, and (c) ambient parameters such as solution temperature, humidity, and air velocity in the electrospinning chamber [5] .

#### 3.1.1 Solution properties

The properties of the polymer solution have the most significant influence in the electrospinning process and the resultant fiber morphology. The surface tension has a part to play in the formation of beads along the fiber length. The viscosity of the solution and its electrical properties will determine the extent of elongation of the solution. This will in turn have an effect on the diameter of the resultant electrospun fibers [4]. However, in roller electrospinning, some solution properties not only determine the morphology of nanofibers but also play an important role on what can be called as feeding in roller electrospinning. Bringing enough polymer solution on the spinable position requires enough viscosity, this process is only necessary in roller electrospinning. This property will be measured using rheometer.

##### 3.1.1.1 Viscosity of the polymer solution

Viscosity, as explain in section 2.1, is one of the most important parameters on roller electrospinning. The viscosity of the solution and its electrical properties determine the extent of elongation of the solution. These have an effect on the diameter and other morphological properties of the resultant electrospun fibers. However, this property has limits, at low viscosity; it is common to find beads along the fibers deposited on the collector. When the viscosity increases, there is a gradual change in the shape of the beads from spherical to spindle-like until a smooth fiber is obtained. High viscosity discourages the bending instability to set in for a longer distance as it emerges from the roller surface. As a result, the jet path is reduced and the bending instability spreads over a smaller area [Mituppatham et. al. (2004)]. This reduced jet path also means that there is less stretching of the solution resulting in a larger fiber diameter. However, when the viscosity is high enough, it may discourage secondary jets from breaking off from the main jet which may contribute to the increased fiber diameter [4] .Therefore, determining the viscosity range of each polymer to be spun is required. There are two most factors that affect the viscosity of the solution; solution concentration and molecular weight.



## **Concentration**

Many studies show that to obtain fibers via electrospinning, the concentration of solution cannot be too low. Via needle spinning, with low concentration of solution, the product includes beads and fibers. The shape of beads changes from spherical to spindle-like and finally uniform fibers with increased diameters by increasing concentration of solution. On the other hand, if concentration of solution is too high, spinning process is difficult because of high viscosity and produced fibers show great diameters. Thus, the optimum concentration of polymer solution should be found for electrospinning process. Researchers also found relationship between solution concentration and fiber diameter as a power law relationship, that increasing concentration of solution, increases the fiber diameter [3].

## **Molecular weight**

Some solution properties such as viscosity and in some extent also surface tension, conductivity and dielectric strength are significantly affected by molecular weight of polymer [12]. And of course, it also affect to electro spinning process and morphology of fibers. Generally, electro spinning can only occur with moderately concentrated solutions, as the process of jet formation relies on the entanglement of polymer chains [14, 15 and 16]. Conventional measures of the extent of the chain overlap and entanglement in solution can therefore be useful metrics in describing the amenability of a given polymer solution to electro spinning. These measures usually involve the quantity  $M_c$  the critical molecular weight at which chain entanglements in solution become significant. Two approaches that address the relationship between the concentration regime and electrospinnability of polymer solutions have been proposed. Both can potentially identify concentration regimes where defect-free continuous nanofibers can electro spun.

### **3.1.1.2 Surface Tension**

Surface tension, more likely to be a function of solvent compositions of the solution plays a critical role in the electro spinning process and by reducing the surface tension of a nanofiber solution fibers can be obtained without beads. Different solvents may contribute to different surface tensions. Generally, high surface tension of a solution inhibits the electrospinning process because of instability of the jets and the generation of sprayed droplets [9]. The formation of droplets, beads and fibers depends on the surface tension of solution. Lower surface tension of the spinning solution helps electrospinning to occur at a lower electric field [12]. However, not necessarily a lower surface tension of a solvent will always be more suitable for electrospinning. Basically, surface tension determines the upper and lower boundaries of the electrospinning window if all other variables are held constant [11, 13 and 10].

### **3.1.1.3 Conductivity/surface charge density**

Polymers are mostly conductive, with a few exceptions of dielectric materials, and the charged ions in the polymer solution are highly influential in jet formation. Solution conductivity is mainly determined by the polymer type, solvent used, and the presence of ionisable salts. It has been found that with the increase of electrical conductivity of the solution, there is a significant decrease in the diameter of the electro spun nanofibers

whereas with low conductivity of the solution, there results insufficient elongation of a jet by electrical force to produce uniform fibers, and beads may also be observed. Hayati [17] have showed that highly conductive solutions are extremely unstable in the presence of strong electric fields, which results in a dramatic bending instability as well as a broad diameter distribution. Generally, electrospun nanofibers with the smallest fiber diameter can be obtained with the highest electrical conductivity and it has been found that the drop in the size of the fibers is due to the increased electrical conductivity. It was observed that the jet radius varied inversely with the cube root of the electrical conductivity of the solution [13, 20, 21, 17-18].

Natural polymers are generally poly-electrolytic in nature, for example, gelatin. The ions increase the charge carrying capacity of the jet, thereby subjecting it to higher tension with the applied electric field. Thus the fiber forming ability of the gelatin is less as compared to the synthetic ones. Zong [18] have demonstrated the effect of ions by adding ionic salt on the morphology and diameter of electro spun fibers and found that with the addition of ionic salts like  $\text{KH}_2\text{P}_04$ ,  $\text{NaH}_2\text{P}_04$ , and  $\text{NaCl}$  it produced bead-less fibers with relatively smaller diameters ranging from 200 to 1000 nm. This approach of increasing the solution conductivity by the use of salt addition has also been used for other polymers such as, PEO[13], collagen type I-PEO[20], PYA [19], polyacrylic acid (PAA) [18], polyamide-6 [22] and others. With the use of salts, the uniformity of fibers increases and there is a decrease in beads generation [3].

### **3.1.2 Process parameters of roller electrospinning**

#### **3.1.2.1 Applied voltage**

A crucial element in electrospinning is the application of a high voltage to the solution. The high voltage will induce the necessary charges on the solution and together with the external electric field, will initiate the electrospinning process when the electrostatic force in the solution overcomes the surface tension of the solution. Depending on the feed rate of the solution, a higher voltage may be required so that the Taylor Cone is stable. The columbic repulsive force in the jet will then stretch the viscoelastic solution. If the applied voltage is higher, the greater amount of charges will cause the jet to accelerate faster. This may result in a smaller and less stable Taylor Cone. As both the voltage supplied and the resultant electric field have an influence in the stretching and the acceleration of the jet, they will have an influence on the morphology of the fibers obtained. In most cases, a higher voltage will lead to greater stretching of the solution due to the greater columbic forces in the jet as well as the stronger electric field. These have the effect of reducing the diameter of the fibers and rapid evaporation of the solvent. When a solution of lower viscosity is used, a higher voltage may favor the formation of secondary jets during electrospinning. This has the effect of reducing the fiber diameter. Another factor that may influence the diameter of the fiber is the flight time of the electrospinning jet. A longer flight time will allow more time for the fibers to stretch and elongates before it is deposited on the collection plate. In this case, at a lower voltage, the reduced acceleration of the jet and the weaker electric field may increase the flight time of the electrospinning jet which may favor the formation of finer fibers. In this case, a voltage close to the critical voltage for electrospinning may be favorable to obtain finer fibers [4]. In an interesting observation, Krishnappa reported that increasing voltage will increased the beads density, which at an even higher voltage; the

beads will join to form a thicker diameter fiber. Similar behavior of applied voltage on fiber diameter is also observed by Larrondo and Manley [24,25]. They have showed the decrease of fiber diameter by roughly half by doubling the applied electric field. Thus, voltage influences fiber diameter, but the level of significance varies with the polymer solution concentration and on the distance between the roller and the collector [26].

### 3.1.2.2 Type of collector [3]

One important aspect of the electrospinning process is the type of collector used. In this process, a collector serves as a conductive substrate where the nanofibers are collected. Generally, aluminium foil is used as a collector but due to difficulty in transferring of collected fibers and with the need for aligned fibers for various applications, other collectors such as conductive paper, conductive cloth, wire mesh[28], pin[29], parallel or grid bar[30], rotating rod, rotating wheel[31], liquid non solvent such as methanol coagulation bath [32] and others are also common types of collectors nowadays.

In the blowing-assisted electro spinning of hyaluronic acid, Wang [28] used two kinds of collector aluminium foil and wire screen and found that a less conductive area of wire screen imposes a negative effect on fiber collection. With less conductive area, there was generation of beaded fibers because of the less surface area. In another study they compared wire screen with aluminium foil and wire screen without aluminium foil in the same conductive area and found that pure wire screen is a better collector for fiber collection because with the use of wire screen the transfer of fibers to other substrates became easy. The fiber alignment is determined by the type of the target/collector and its rotation speed [33].

The generated nanofibers are deposited on the collector as a random mass due to the bending instability of the highly charged jet [34, 35]. Several research groups have demonstrated the use of a rotating drum or a rotating wheel-like bobbin or metal frame as the collector, for getting aligned electrospun fibers more or less parallel to each other [40, 41, and 42]. Several types of split electrodes have been used for getting aligned nanofibers and typically such collectors consist of two conductive substrates separated by a void gap where aligned nanofibers are deposited[38,39].

### 3.1.2.3 Velocity of the collector

The velocity of the collector determines the areal weight of the nano-fiber fabric. If the velocity of the collector is low, the areal weight is expected to be large. This also affects to quality of nanofibers membrane as non-fibrous area [3].

### 3.1.2.4 Roller to collector distance

The distance between the roller and the collector could be recognized as another approach to control the fiber diameters and morphology. It has been found that a minimum distance is required to give the fibers sufficient time to dry before reaching the collector, otherwise with distances that are either too close or too far, beads have been observed[47,48,43]. The effect of roller and the collector distance on fiber morphology is not as significant as other parameters and this has been observed with electrospinning of PVA[52], gelatin[47], chitosan [43] and poly (vinylidene fluoride) [44].

It has been reported that flatter fibers can be produced at closer distances but with increase in distance rounder fibers have been observed with the spinning of silk-like polymer with fibronectin functionality [53]. For polysulfone, closer distances to the collector have yielded smaller fibers [49]. One important physical aspect of the electrospinning nanofibers is their dryness from the solvent used to dissolve the polymer [39]. Thus, there should be optimum distance between to the collector which favours the evaporation of solvent from the nanofibers [3].

### **3.1.2.5 Speed of rotation of roller**

The roller speed of rotation is one of the important parameters of roller electrospinning, roller rotation brings the polymer solution to the spinnable position. High speed of rotation brings more polymer solution on the surface of the roller, therefore, more jets are formed. The amount of solution on top of the roller depends mainly on the roller speed of rotation and solution's viscosity.

### **3.1.2.6 Ambient parameters**

Studies have been conducted to examine the effects of ambient parameters (i.e. temperature and humidity) on the electrospinning process. Mit- Uppatham [51] have investigated the effect of temperature on the electrospinning of polyamide-6 fibers ranging from 25 to 60 DC and found that with increase in temperature, there is a yield of fibers with decreased fiber diameter, and they attributed this decline in diameter to the decrease in the viscosity of the polymer solutions at increased temperatures. There is an inverse relationship between viscosity and temperature.

The variation in humidity while spinning polystyrene solutions has been studied and shows that by increasing humidity there is an appearance of small circular pores on the surface of the fibers; further increasing the humidity leads to the pores amalgamation [45]. It has been found that at very low humidity, a volatile solvent may dry out rapidly and the evaporation of the solvent is faster. Sometimes the evaporation rate is so fast than compared to the removal of the solvent from the tip of the needle and this would create a problem with electrospinning. As a result, the electrospinning process may only be carried out for a few minutes before the needle tip is blocked [50]. It has also been suggested that the high humidity can help the discharge of the electro spun fibers [54,46]. It can be noticed that ambient parameters also affect the electrospinning process and electro spun fibers.

## **3.2 Dependent parameters of roller electrospinning [3]**

### **3.2.1 Density of Taylor cones (D)**

In contrast with the needle technique, which only has one Taylor cone during spinning process, in needleless technique a number of Taylor cones (N) appear on spinning area during spinning process. The density of Taylor cones can be determined from a camera record [5] as the number of Taylor cones N per area ( $m^{-2}$ ). Density of jets is one important parameter in the needleless spinning process. It has relation with solution properties, field strength, the spinning performance and the average life time of jets.

To determine the density of cone, the spinning process will be recorded by camera. A number of pictures were taken from the camera record. The number of Taylor cones (N) was counted from these pictures. The density of Taylor cones (D) will be calculated as the ratio of number of Taylor cones (N) to the spinning area (A) which is determined as one third of surrounding area of the roller. So we have:

$$D = \frac{N}{A} \quad (\text{m}^{-2}) \quad (3.1)$$

Where:  $A = \frac{\pi \times d \times l}{3} \quad (\text{m}^2) \quad (3.2)$

d is diameter of the roller (m).

l is length of the roller (m).

### 3.2.2 Life time of jet

Life time of jet can be defined as the period of time from the point that the jet appear to the point that the jet disappear [62]. Of course in needleless technique, during spinning process, there is not only one jet, there are a number of jets, and the life time of every jet is different from that of the others. It depends on polymer solution, on environment, on position of the jet on the roller electrode, on number of jets also ... etc. so the life time of jet in one process can be that determined by calculating average life time of different jets in different position in different time during spinning process as described by the author [62, 151]. Similar to the parameter of needle electro spinning, fibers diameter of needleless electro spinning is an important parameter to evaluate the quality of nanofibers membrane.

### 3.2.4 Spinning performance (SP) [3]

Spinning performance or throughput is one of the most important characteristics of needleless electrospinning. It describes the amount of nanofiber material produced by the specific spinning device in time. In contrast with the needle electro spinning, the spinning performance is a dependent variable in needleless electro spinning. It can be determined from the mass of nanofibers produced in one minute recalculated per one meter long roller spinning electrode. In praxis, spinning performance is recalculated from area weight of produced nanofiber layer as follows:

$$SP = \frac{G \cdot v \cdot l_f}{l_r} \quad , \quad [\text{g}/\text{min}/\text{m}] \quad (3.3)$$

Whereas SP is spinning performance or throughput, it has unit as g.m/min

G is weight of nanofibers membrane per area in  $\text{g}/\text{m}^2$

v is velocity of running collected fabric, in m/min.

$l_f$  is the width of nanofibers membrane on collected fabric, in m.

$l_r$  is the length of spinning roller, in m.

### 3.2.5 Spinning performance per cone

Spinning performance per cone (SPC) is the spinning ability of one jet during the spinning process. It can be determined by amount of polymer passing through one Taylor cone in time. It has strong relation with throughput parameter.

$$SPC = \frac{SP \cdot l_r \cdot 60}{N_c} \quad [\text{g/h}] \quad (3.4)$$

Whereas SP is spinning performance or throughput (g/minlm), and  $l_r$  is the length of spinning cylinder (m),  $N_c$  is number of Taylor cones during the spinning process.

### 3.2.6 Non-fibrous area (NFA)

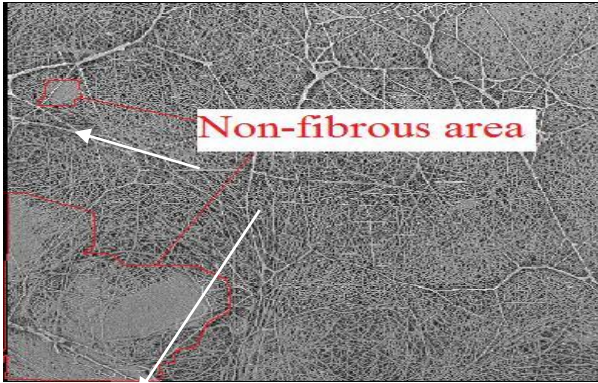


**Figure 3.1:** Non-fibrous areas [3].

The other common property for textile materials is porosity or nonfabrious area. It is important to analyze this property if the quality of nanofiber membrane has to be estimated. Nonfabrious area is the reflection of the spinning process. The NFA is the area fraction of non-fibrous area in membrane to total area of product. It is expressed as percentage, or dimensionless. This can be calculated according to formula below:

$$NFA = \frac{\text{Total non fiborous area}}{\text{total area of nanofiber memberane}} * 100 [\%] \quad (3.5)$$

To measure non-fibrous area, SEM pictures of product will be taken. From these pictures, non-fibrous area can be measured on surface of sample (see figure 2.3). Then measure total area of sample. And then use equation 2.9 to calculate non-fibrous area.

### 3.2.7 Fibers diameter

Similar to the parameter of needle electro spinning, fibers diameter of needleless electro spinning is important parameter to evaluate the quality of nanofibers membrane. The method to determine this parameter is the same to both products of needle and needleless electrospinning. The formula shows the way to calculate the value of this parameter.

$$d_{f(\text{avg})} = \frac{\sum n_i d_i}{\sum n_i} \quad (3.6)$$

$d_i$  is fibre diameter or size of bead (nm)

$n_i$  is number of elements of the group  $d_i$ ,

$d_{f(\text{avg})}$  is average diameter (fibers or beads)

### 3.2.8 Fibers diameter distribution

The difference in fibers diameter or fibers diameter distribution can be shown by the fraction of groups of diameter or in deviation value. The smaller of deviation the bigger number of the nanofibers had their diameter closes to the others. The standard deviation can be calculated using the formula in equation 2.11 and equation 2.12:

$$\sigma = \sqrt{\frac{1}{N} \sum_1^N (x_i - \mu)^2} \quad (3.7)$$

$$\mu = \frac{1}{N} \sum_1^N x_i \quad (3.8)$$

$\sigma$  is standard deviation

$N$  is number of elements (measured nanofibers)

$x_i$  is nanofiber diameter

$\mu$  is Average of nanofibers diameter

## Chapter 4 : Experimental

This chapter explains, in details, the experiments that were carried out on this work, the methods that were used to perform the experiments; stating the dependent parameters and the independent parameters. The parameters mentioned in this chapter are the parameters of the interest due to the focus of this work, while parameters explained in chapter 3 are parameters of roller electrospinning, hence, they are still part of this work. The chapter also clarifies the used materials for the experiments.

### 4.1 Experiments performed

4.1.1 The thickness of the layer of the polymer solution onto the surface of the rotating roller was evaluated.

- ⊕ Independent parameters
  - Concentration of polymer solution
  - Roller rotational speed (rpm)
- ⊕ Dependent parameter
  - Thickness of the layer of polymer solution onto the rotating roller

### 4.1.2 Roller electrospinning

- ⊕ Independent parameters
  - Concentration of the polymer solution
  - Roller rotational speed (rpm)
  - Addition of sodium chloride salt
- ⊕ Dependent parameters
  - Throughput
  - Throughput per jet
  - Number of Taylor cones
  - Current
  - Current per jet

## 4.2 Material

In this work Polyvinylalcohol (PVA) was used in different concentrations as the material for the experiment. The 16% PVA water solution (brand name of SLOVIOL R) produced by Chimicke Zavody Novaky from Slovak Republic was used to prepare various concentrations of the solutions proportional to sodium chloride as the conductive additive and water as solvent. The prepared PVA solutions are tabulated in the table below.



**Table 4.1:** Prepared solutions for experiment.

PVA concentration (%) in solution	NaCl concentration (%) in a solution
6	0.0
7	
9	
12	
15	
12	0.1
	0.2
	0.5
	1.0

The properties, such as zero shear viscosity, surface and conductivity of the solutions in table 4.1 were measured. Reometer ROTOVISCO RV1 instrument, set to reach shear rate of 6000 /s in 30s was used to measure the zero-shear viscosity of the above tabulated solutions. The property, surface tension was measured using Tensiometer (KRÚS) and then the conductivity was measured by conductivity instrument OK-102/1 Radelkis. The results will be found at the next chapter.

## 4.3 Method

### 4.3.1 Film thickness measurement

Figure 4.1 show the image of the system used to measure thickness of the layer of the PVA solutions onto the roller surface. Number (1) is the rotating roller with a diameter of 20.0 mm, driven by the electrical motor, (2) is the pan filled with polymer solution, (3) is the micrometer and (4) is the supporting stand.

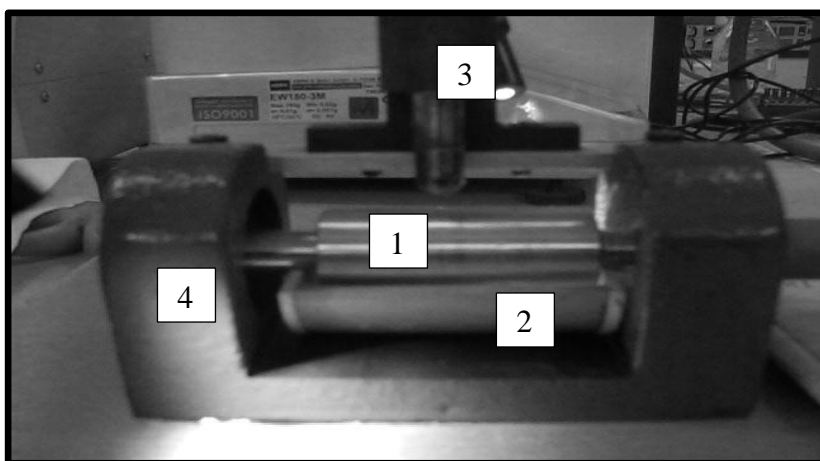


**Figure 4.1:** Cylinder (diameter of 20 mm) immersed into the polymer solution.

- The polymer solution (6% PVA) was poured into the pan, until the roller was immersed into the solution.
- Then the motor was switched on, picking up the polymer solution from the pan starting with rotational speed of 0.5 rpm.
- And then the micrometer was turned or screwed down (into the page) until it touched the film onto the roller, and then the thickness of the polymer solution layer was recorded.
- The micrometer was screwed out of the page and cleaned. These steps, involving micrometer were repeated until the desired measurements were recorded.

These steps were repeated for roller rotational speeds after 0.5 to 1.0, 1.5, 2.0, 3.0, 4.0 and 5.0 rpm. And then the measurements were done for each of the solutions tabulated in table 4.1. The results follow in chapter 5.

**4.3.2 Roller electrospinning**

After the solutions mentioned in section 4.2 were prepared and their properties were measured, they were then spun into nanofibers by the technology of roller electrospinning.

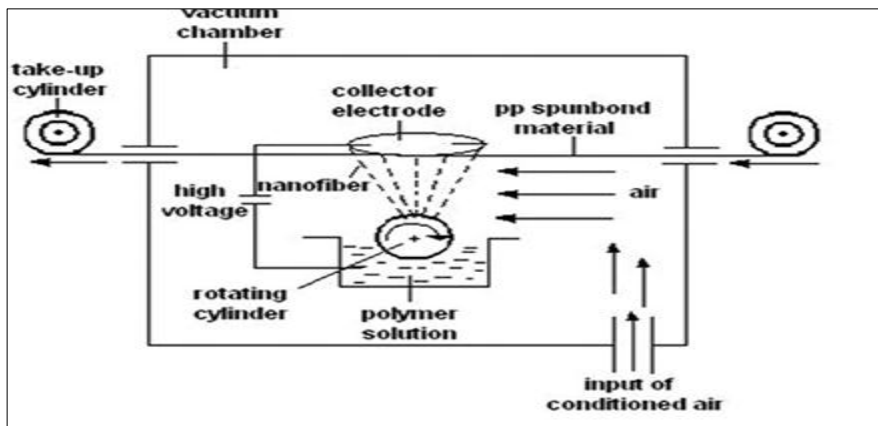


**Figure 4.2:** Schematic diagram of roller electrospinning set up [58].

The electrospinning apparatus set up in series connection with the electronic device to measure the output voltage from spinning section. The external video camera was set in position to observe spinning process.

**Table 4.2:** Spinning conditions.

Applied Voltage (kV)	Distance Between Electrodes(mm)	Relative Humidity (%)	Temperature(C°)	Roller Speed(rpm)	Fabric Speed (cm/min)
55	120	30	25	2.5	10

The spinning experiments were carried out with the aims of finding some different factors affecting electrospinning. First, to find the effect of roller speed to roller electrospinning, therefore, the spinnable 12%PVA was spun in different roller speed (1.5, 2, 3, 4 and 5rpm). Second, to find effect of concentration, this was carried out by spinning PVA solutions with different concentrations (6%, 7%, 9%, 12% and 15%) at constant roller’s rotations per

minute (2.5 rpm). Third, is to obtain the effect of sodium chloride in electrospinning. 12% PVA solutions containing 0.1%, 0.2%, 0.5% and 1.0% of sodium chloride were spun at constant roller's rotation per minute (2.5 rpm).

## Chapter 5 : Results and discussions

This chapter contains the results of all the experiments carried out for this research work. The chapter also includes the discussions about the results. Tables and graphs are used to analyze the results enclosed in this chapter.

### 5.1 Viscosity, conductivity and surface tension

This section contains properties of the PVA solutions prepared for the use in the experiments of this work.

**Table 5.1:** Viscosity, surface tension and conductivity of different PVA solutions.

Sample	Viscosity(Pa s)	Surface tension (mN/m)	Conductivity (mS/cm)
6%PVA	0.03565	45.8	0.432
7%PVA	0.05669	45.4	0.44
9%PVA	0.115	46.2	0.596
12%PVA	0.356	46.8	0.66
15%PVA	0.836	46.7	0.792
12%PVA+			
0.1%NaCl	0.367	46.5	2.24
0.2%NaCl	0.348	46.3	4.08
0.5%NaCl	0.345	46.5	8.32
1.0%NaCl	0.381	46.4	13.2

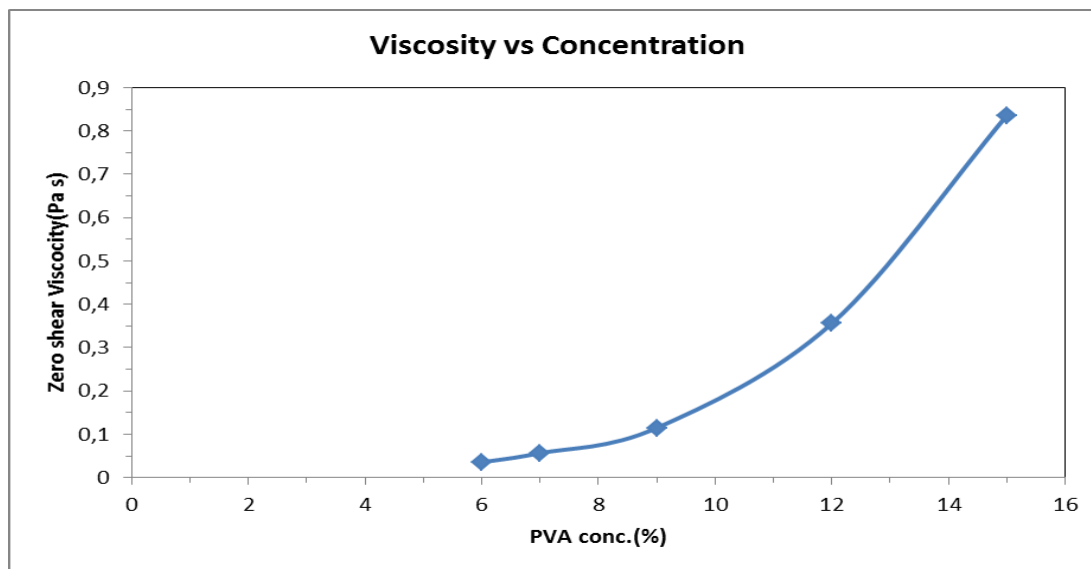


**Figure 5.1:** Graph of zero shear viscosity as a function of concentration (%).

The graph in figure 5.1 shows that zero shear viscosity of PVA solution increases with the increase of its concentration. The graph indicates the exponential relationship ( $R^2$  equal to 99.57%) between zero shear viscosity and concentration of the polymer solution.

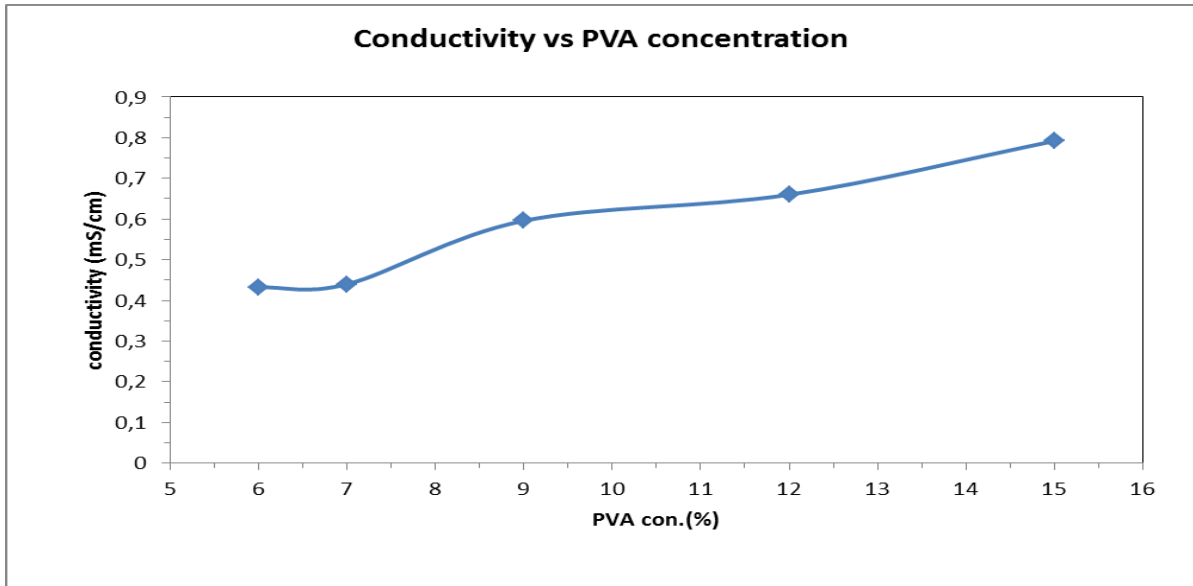


**Figure 5.2:** Graph of conductivity (mS/cm) at different PVA concentration (%).

The graph shows that conductivity of the PVA solution is directly proportional to the PVA concentration.

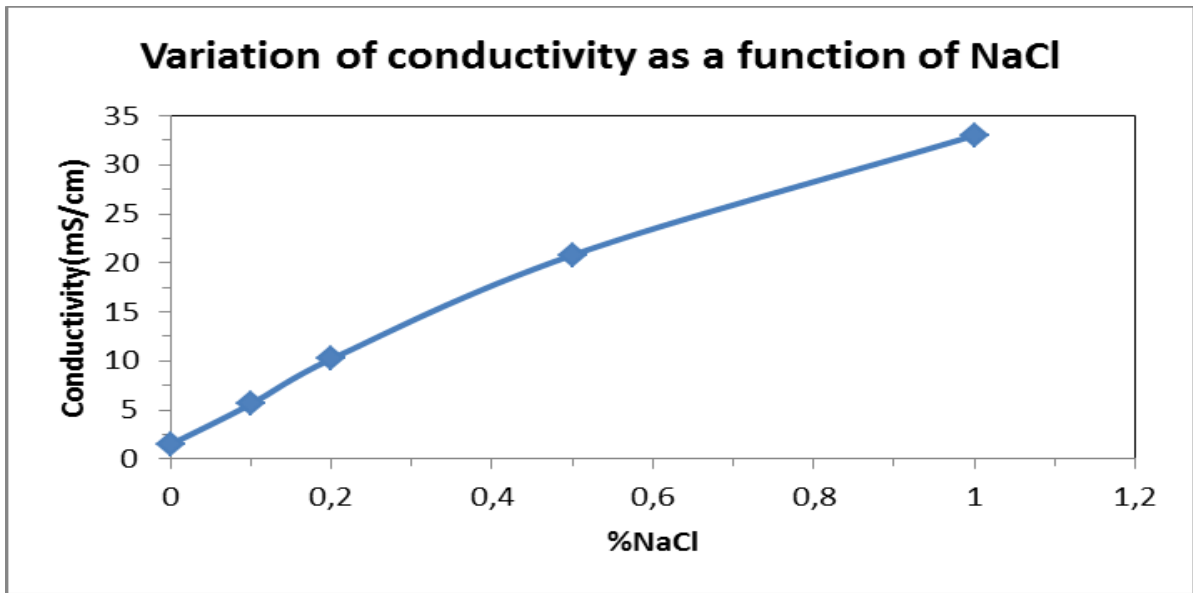


**Figure 5.3:** Graph of conductivity (mS/cm) of 12% PVA with various NaCl (%).

Graph in figure 5.3 shows the increase in conductivity of the PVA solution as the results of increasing the concentration of NaCl salt in the solution.

**Discussion of section 5.1**

The viscosity-concentration exponential relationship shown in figure 5.1 is an evidence of equation 2.7; this equation means that the relative viscosity and solution concentration has exponential relationship.

The experiments confirmed the linear relationship between the conductivity and the concentrations of the solutions for small concentrations. However, the effect of PVA concentration on the conductivity of the solution is significantly small when it is compared to the changes brought by sodium chloride salt on the solution. The idea is witnessed by the graphs in figure 5.2 and figure 5.3 which show that the slopes are equal to 0.0405 and 12.485, respectively. This is due to the fact that dissociation of sodium chloride provides sodium ions which are regarded as good charge carriers.

**5.2 Thickness of the layer of PVA solution on the roller**

This section (5.2) contains the results, observations and discussions of the investigation of thickness of the layer of the PVA solution on the spinning roller. The table tabulates the average thickness of layer of PVA solution on top of the spinning roller.

After the roller, which is partially immersed in the polymer solution, rotates at constant angular velocity, polymer solution-film around the roller is created by the interactions among the viscous, inertia and surface tension forces of the polymer solution. At the moment of the polymer-film formation, the film thickness develops because of viscous and inertia forces.

**Table 5.2:** Thickness of the layer (mm) of PVA solution as the function of roller speed.

		Roller speed(rpm)						
		0.5	1.0	1.5	2	3	4	5
Average Thickness of the layer (mm)	Sample							
	6%PVA	0.033	0.053	0.058	0.68	0.07	0.075	0.09
	7%PVA	0.04	0.045	0.074	0.065	0.099	0.102	0.112
	9%PVA	0.044	0.081	0.097	0.104	0.105	0.127	0.154
	12%PVA	0.107	0.142	0.189	0.206	0.254	0.286	0.309
	15%	0.177	0.264	0.344	0.395	0.497	0.544	0.6
	12%PVA +							
	0.1%NaCl	0.131	0.191	0.202	0.265	0.328	0.372	0.375
	0.2%NaCl	0.143	0.209	0.249	0.22	0.27	0.321	0.354
	0.5%NaCl	0.099	0.148	0.167	0.166	0.223	0.255	0.261
	1.0%NaCl	0.121	0.159	0.199	0.224	0.285	0.306	0.347

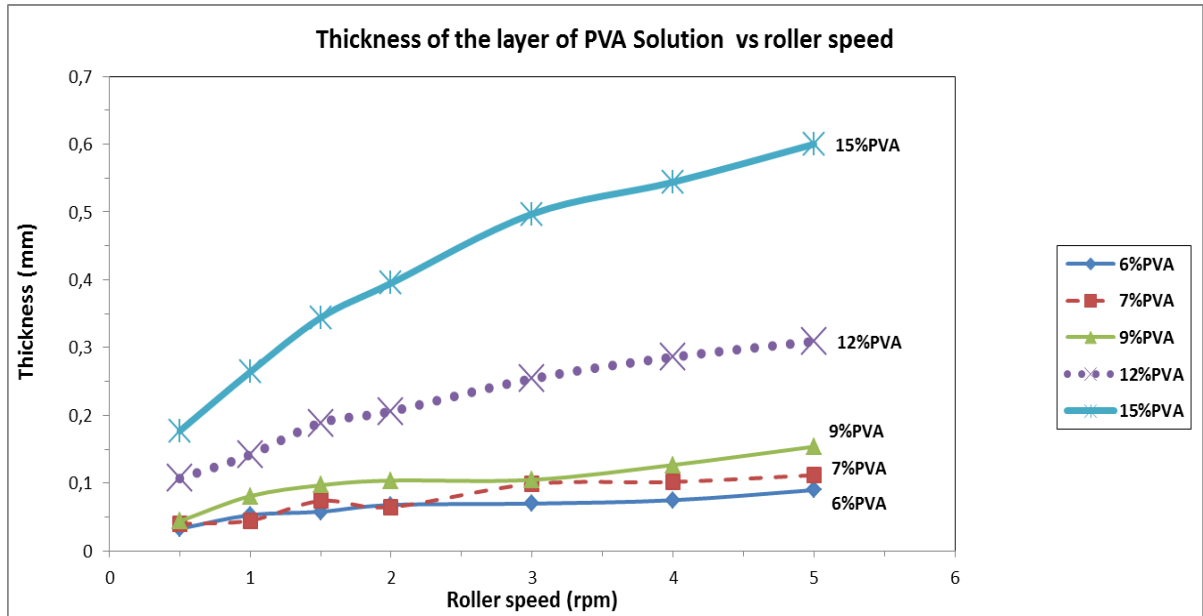


**Figure 5.4:** Graph of thickness (mm) of the layer of PVA solutions (with different concentrations) on the roller surface as the function roller’s rotation (rpm).

The above figure 5.4 shows that the increase in speed of the roller increases the amount of polymer solution taken onto the surface of the roller. The graphs in figure 5.4 show the relationships as power (power less than 1) regression, with R-squared greater or equal to 0.91.

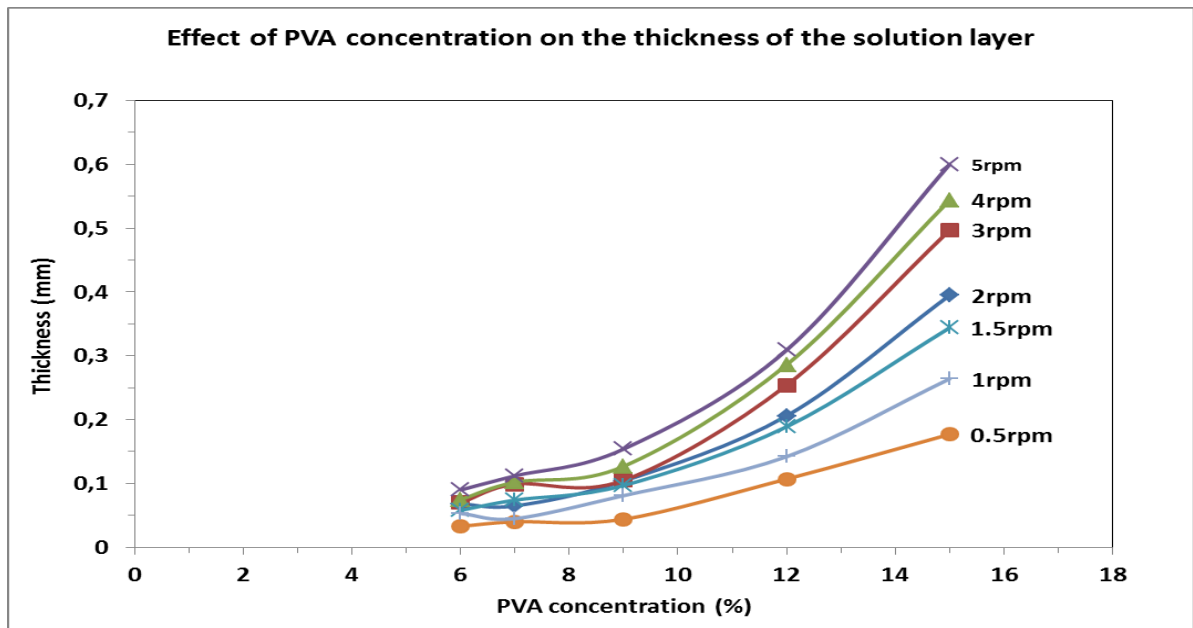


**Figure 5.5:** The graph shows the effect of PVA concentration (%) on the thickness of the layer (mm) of the PVA solution onto the spinning roller.

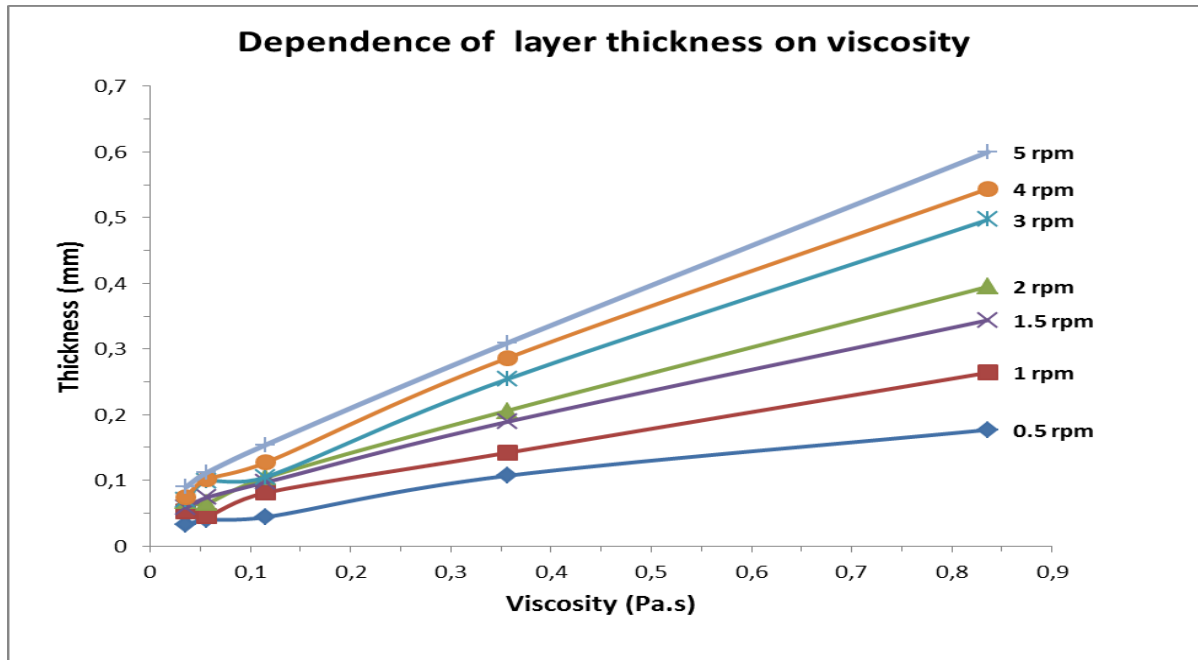


**Figure 5.6:** The graphs of thickness (mm) of the layer of PVA solutions as the function viscosity (Pa.s) at indicated roller speeds.

Figure 5.5 contains the graphs that show that the layer thickness on the roller surface is proportional to the viscosity of the polymer solution. The increase in PVA concentration causes the exponential increase on the thickness of the layer of the polymer solution onto the roller. The graphs in figure 5.6 show the dependence of thickness of the layer of polymer solution on viscosity of the solution at constant angular speed of spinning roller. The relationship is mostly considered as linear ( $R^2$  greater than 0,99).

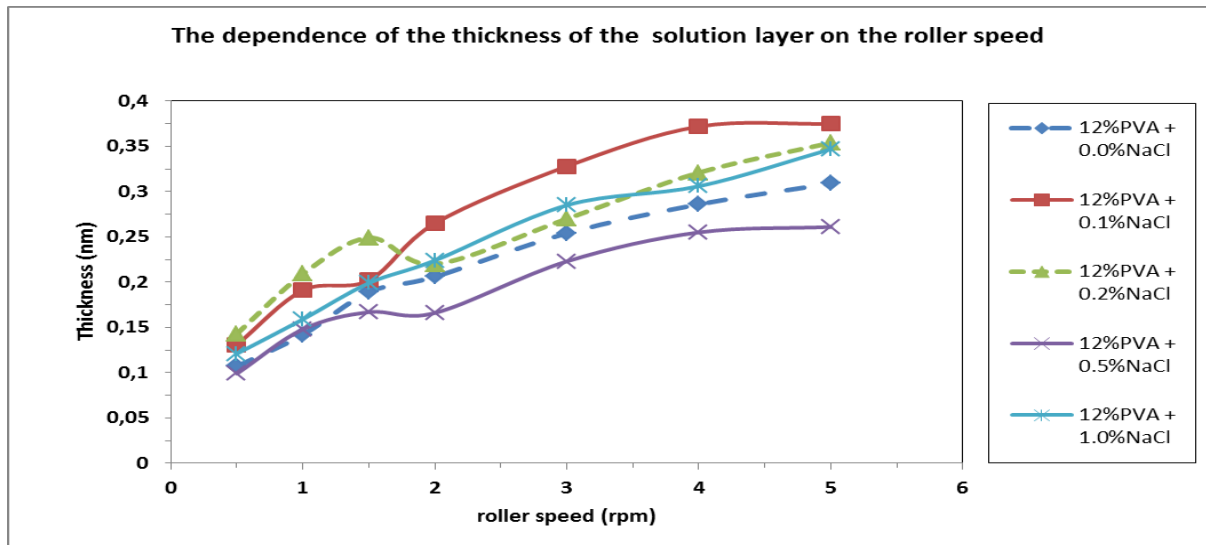


**Figure 5.7:** Graph of thickness (mm) of the layer of PVA solutions (with different NaCl concentrations) on the surface of the roller at different roller speed (rpm).



The thickness of the layer of the solution with the small (approximately 0.1%) percentage of sodium salt in the graph above shows small effect on the layer thickness on the roller. The thickness of the layer of 12%PVA solution with various NaCl salt concentrations is comparable to 12%PVA solution without salt.

### **Discussion of section 5.2**

The graphs in figure 5.4 prove that the theory about the relation between the thicknesses of the layer of polymer solution onto the rotating roller, discussed in chapter 2 is valid since equation 2.1 and equation 2.3 state that the thickness of the layer is directly proportional to the square root of the rotational speed. The thickness increases from slow rotations to high rotations, since if the roller is rotating slowly it gives enough time to gravitational force to act against the upward motion of the polymer solution, therefore less polymer reaches the top (at 90°) of the roller, whereas more polymer solution reaches the top of the roller if the roller rotates with high speed. High angular velocity also means large inertia force, which induces more momentum transfer into the film flow.

The experimental results also show that the polymer solution reaches the top (90°) of the rotating roller is highly dependent on the concentration of the polymer solution. Figure 5.5 indicates that the increase in concentration of polymer solution causes the noticeable increase on the thickness of the layer of polymer solution on top (90°) of the rotating roller. The relationship between layer thickness and concentration is exponential.

The graphs in figure 5.6 indicate that the thickness of the layer of polymer solution is linearly dependent on the viscosity of the polymer solution. The second best relationship mathematical prediction is that the thickness is proportional to the square root of the viscosity. The idea of considering the correlation as linear differs from the theories in chapter 2 which suggested that the thickness of the layer of the polymer solution is directly proportional to the square root of the solution viscosity.

## **5.3 Roller Electrospinning**

This chapter contains the results and analysis of the roller electrospinning of the polymer solutions used to investigate parameters affecting layer thickness onto the electrospinning roller. After the polymer solution is brought on top of the spinning roller, the spinning starts, provided that the solution is spin-able. The spinning process and effects of parameters in question are indicated in the graphs contained in this chapter. The current-test method was used to analyze the electrospinning process; the current in the graphs indicate the amount of the polymer solution from the roller to the collector.

### **5.3.1 Effect of concentration on roller electrospinning**

In this section, results of spinning PVA solutions of different concentrations are contained. The angular speed of the roller used was 2.5rpm.

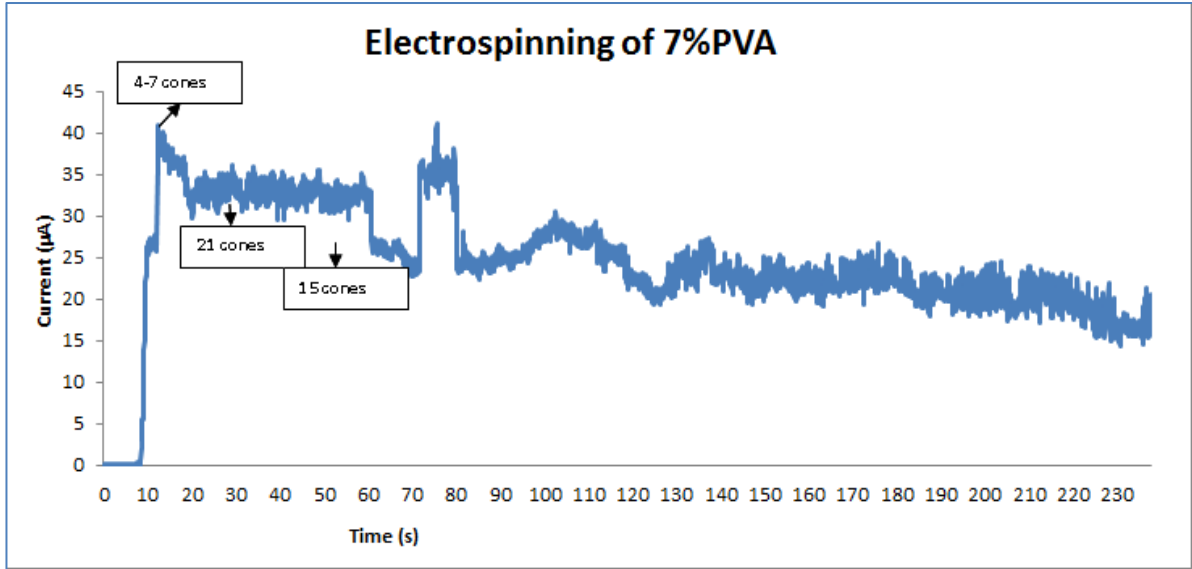


**Figure 5.8:** Graph of electrical current ( $\mu\text{A}$ ) in electrospinning of 7% PVA solution versus time (s).

The graph above shows the current measured during the spinning of 7%PVA solution. It indicates high current at the beginning, and then a decrease as the time goes by. The spinning started with 4 Taylor cones in approximately 3 seconds. High number of Taylor cones, then polymer jets was observed in the beginning of the process, and then decreased to zero as time was progressing.

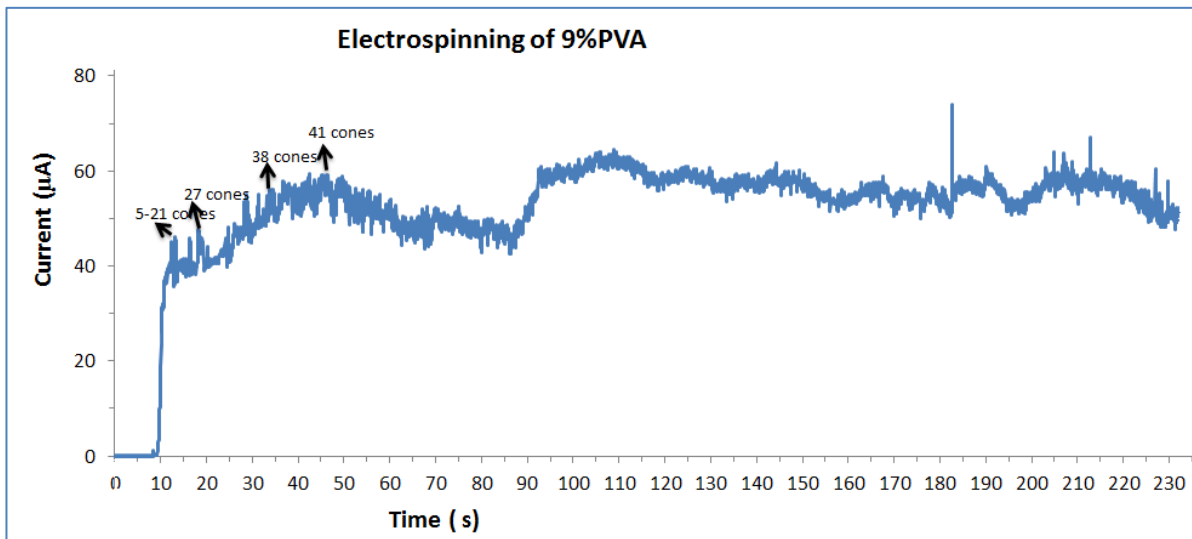


**Figure 5.9:** Graph of electrical current ( $\mu\text{A}$ ) in spinning of 9% PVA solution versus time (s).

The graph in figure 5.9 shows the current flowed through the spinning system during spinning of 9%PVA solution. The first 5 Taylor cones were formed approximate 3 seconds,

and then all other Taylor cones followed as indicated in in figure 5.9. And then spinning reached the stable state i.e. the number of Taylor cones was not changing.

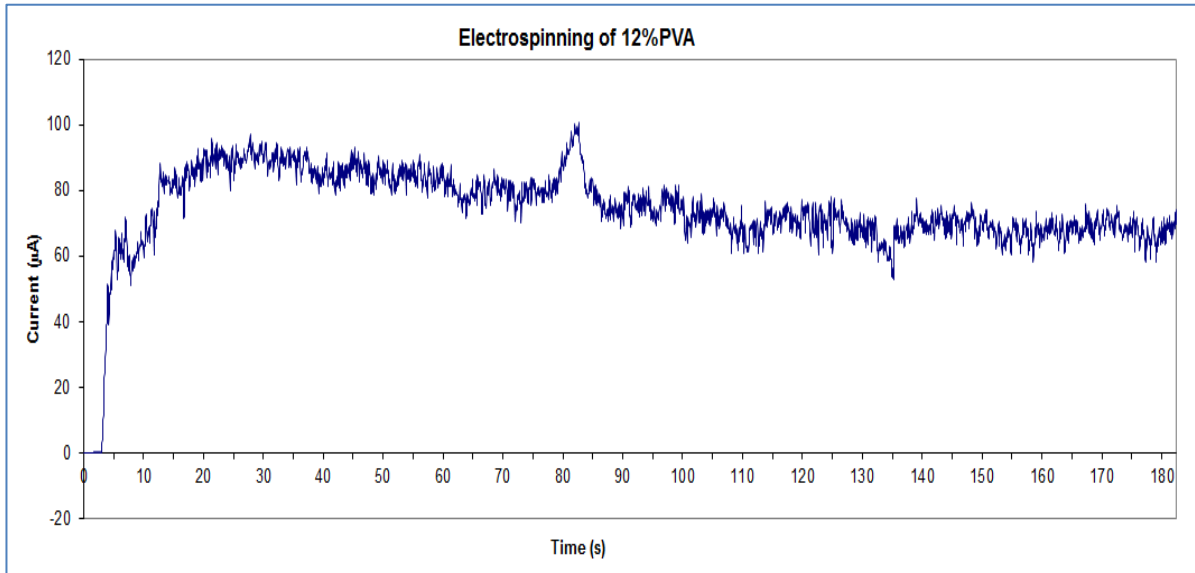


**Figure 5.10:** Graph of electrical current ( $\mu\text{A}$ ) in electrospinning of 12% PVA solution versus time (s).

The formation of the first Taylor cones started in approximately 1-2 seconds, followed by the rapid increase of the number of Taylor cones reaching 70 Taylor cones in 50 seconds. The graph in figure 5.10 shows 80-85  $\mu\text{A}$  of current flow in first 60 seconds of the spinning, which indicates amount of polymer solution that was transported from spinning roller to the collector.

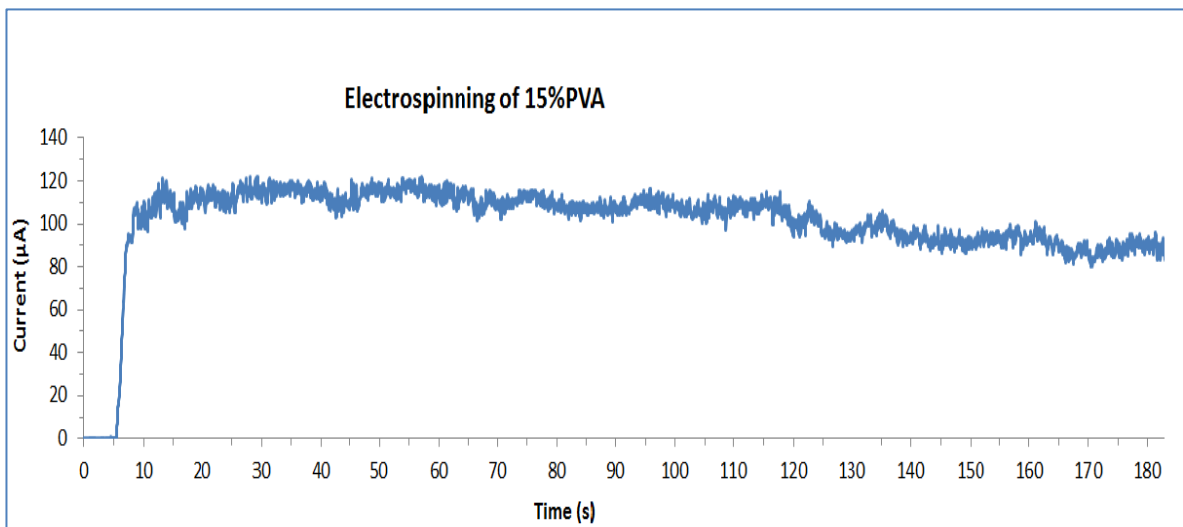


**Figure 5.11:** Graph of electrical current ( $\mu\text{A}$ ) flowing through the system during electrospinning of 15% PVA solution versus time (s).

The graph in figure 5.11 shows the current flowing through spinning system during the electrospinning of 15%PVA solution. The first cone appeared in 2 seconds after switching on the voltage. The number of Taylor cones increased rapidly reaching approximately 95 in 30 seconds. The spinning was characterized by high cone density. The graph shows that spinning reached stability after 120 seconds.

The table below, table 5.3 tabulates the analysis of the properties of roller electrospinning. They are all the results of changing concentration of PVA solution; i.e. 6, 7,9,12 and 15%PVA. The properties were either calculated or visually observed.

**Table 5.3:** The table of PVA concentration-dependent parameters in electrospinning.

Sample	Avr. Current (μA)	Std.dev (μA)	Fabric Throughput (g/min/m)	number of Taylor cones	Throughput/jet (g/min/m)	Current per jet (μA)	Starting of Taylor cones (sec)
6%PVA	-	-	0	0	0	-	-
7%PVA	24	7.2	0	15	0	1,6	3
9%PVA	54	6.4	0,17	40	0,0044	1,3	3
12%PVA	89	12.4	1.09	90	0,0121	0,9889	1,35
15%PVA	100	20.3	1,21	95	0,0127	1,05	2

The following graphs provide understandable analysis of the properties in table 5.3 as the function of changing the concentration of the PVA solution.

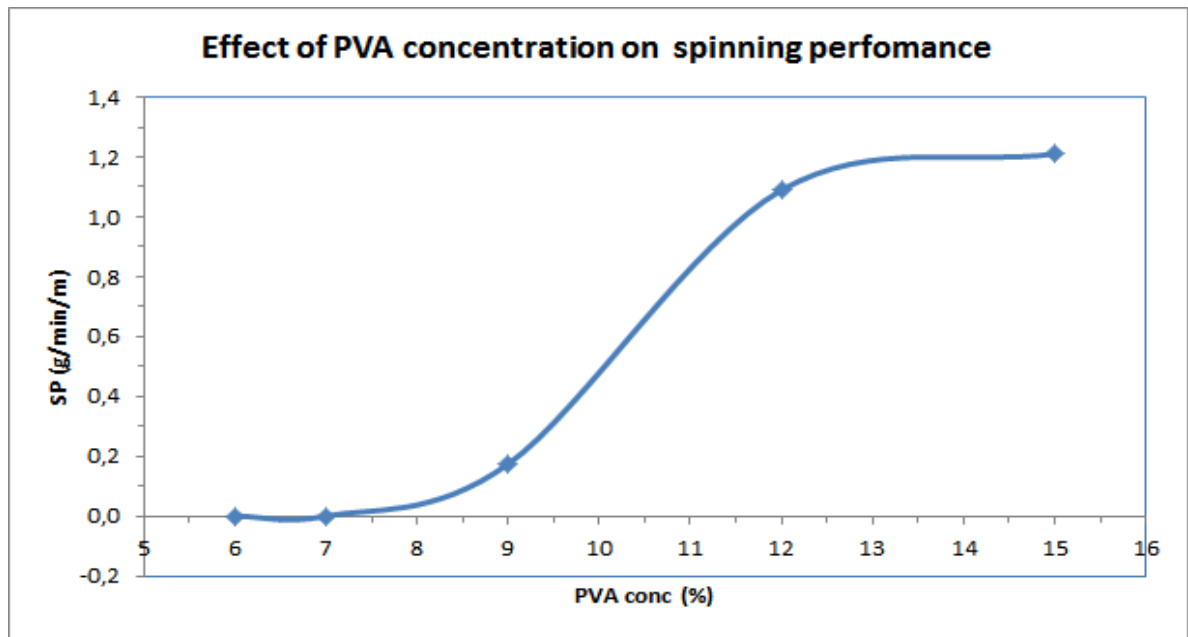


**Figure 5.12:** Graph of spinning performance SP (g/min/m) as a function PVA concentration (%).

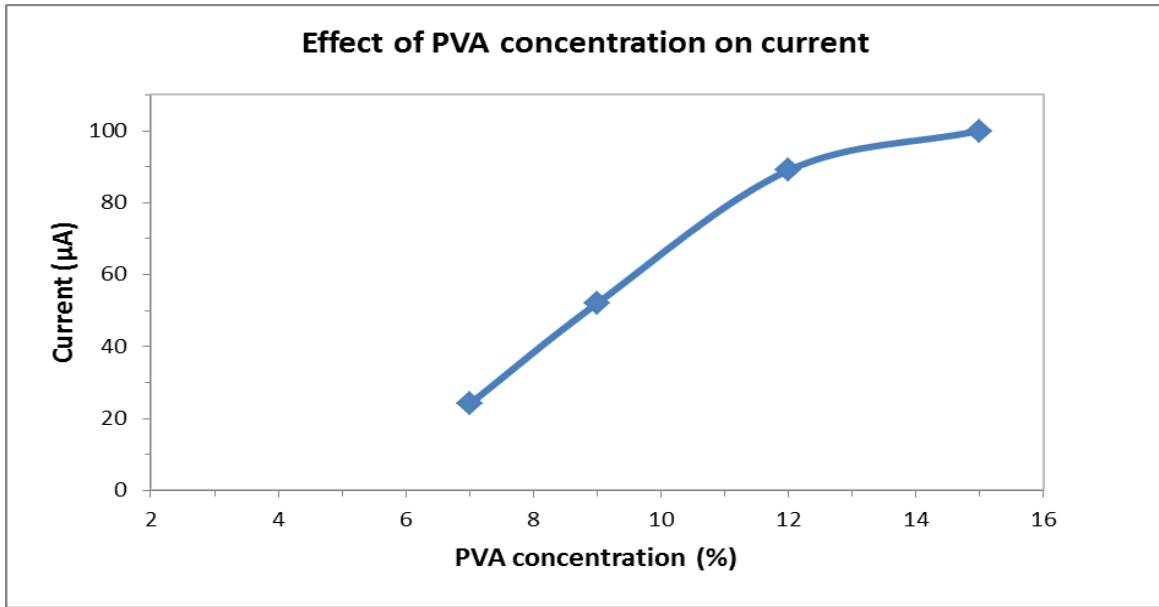


**Figure 5.13:** Graph of flowing current (µA) in the spinning system versus PVA concentration (%).

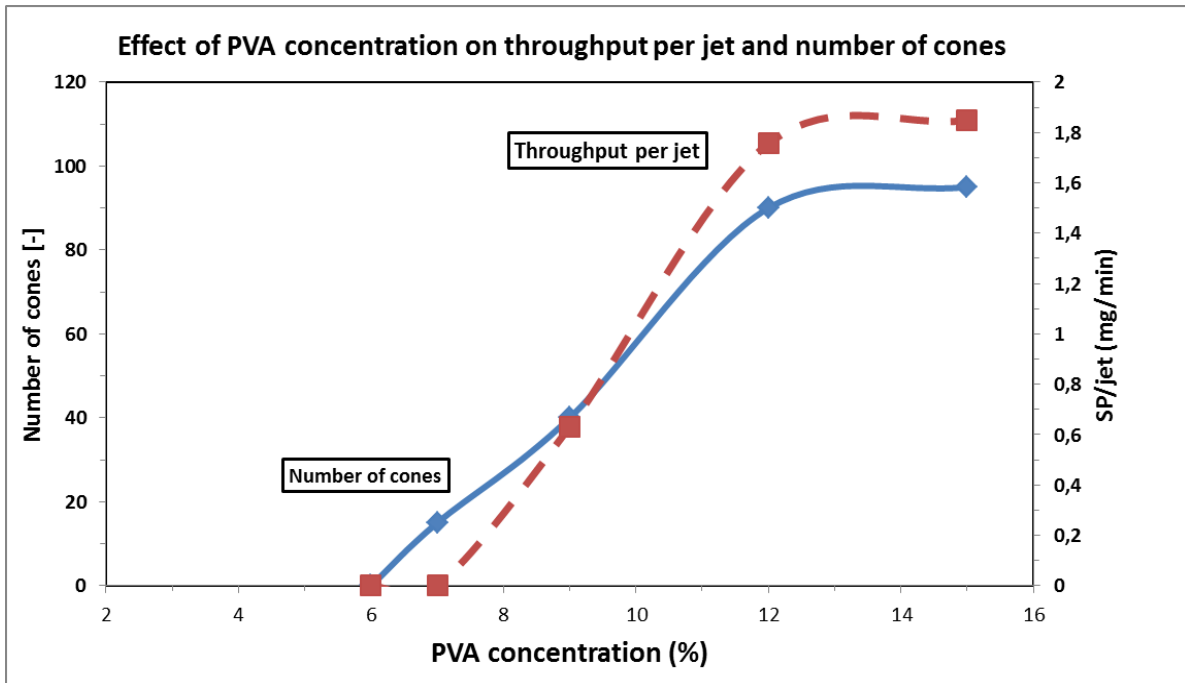


**Figure 5.14:** Graphs show the dependence of number of Taylor cones and throughput SP per jet (mg/min) on the PVA concentration (%).

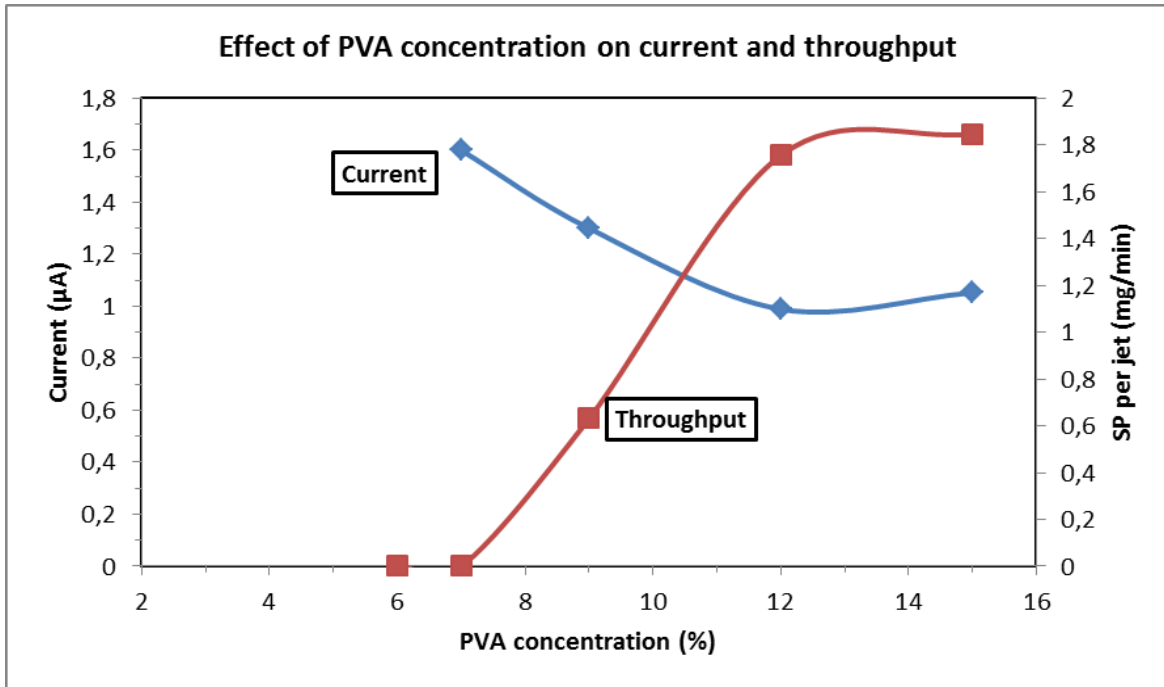


**Figure 5.15:** Graphs show the dependence of current ( $\mu\text{A}$ ) and throughput SP per jet ( $\text{mg}/\text{min}$ ) on the PVA concentration (%).

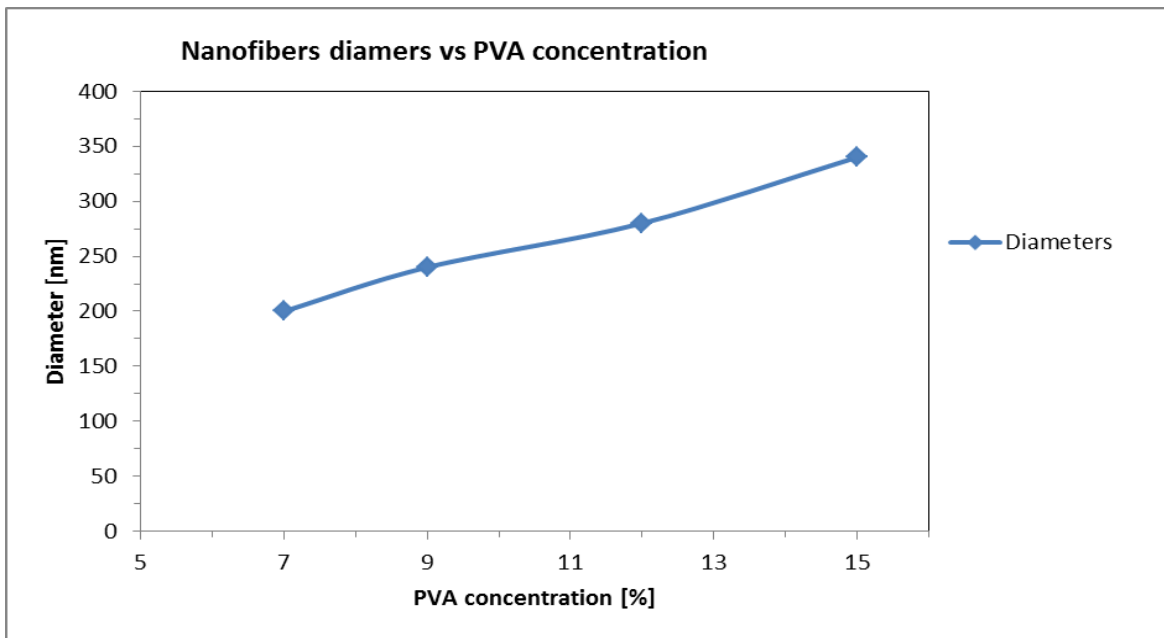


**Figure 5.16:** The graph of nanofiber (nm) diameters vs concentration of polyvinyl alcohol (%).

Graph in figure 5.15 shows a diameter of nanofiber is linearly directly proportional to the concentration of the polyvinyl alcohol.

### Discussion of section 5.3.1

The results in tables and graphs form has shown that increasing the concentration of PVA solution results in increasing the spin ability of PVA solution. Solutions with low viscosity are difficult to be spun .i.e. 6%PVA solution was not spin-able, not even a single cone was observed during the trial to spin this solution; this was due insufficient viscosity, meaning that there was small interaction between polymer micromolecules, the minimum forces are required to keep the molecules together to form cones and jets. Increasing the concentration from 6% to 7%PVA enable spinning of this solution, but the formed Taylor cones were much less when compared to the other solutions with higher concentrations. Theoretically, an increased in the concentration will result in greater polymer chain entanglements within the solution which is necessary to maintain the continuity of the jet during electrospinning. The further increase in concentration improved the spinning parameters and material properties. It was observed during the electrospinning that increasing concentration of the solution shorten the time for first cone(s) appearance. This is the time it took the first cone(s) to be formed after switching on the voltage.

Plotted graph in figure 5.11 indicates that an increase in concentration of the solution cause an increase in spinning performance, this is due to the increase in solution jets, which influences the areal density of the material. Figure 5.12 provides proof that shows an increase in current flowing through the system is as a function of an increase in solution concentration. The increase of average current in this experiment was due to the increase in number of Taylor cones as shown in figure 5.13. Graphs in figure 5.14 show that the solution concentration is proportional to the spinning performance per jet and inversely proportional to the current per jet, it means, increasing the concentration of the solution causes rapid increase in the number of Taylor cones. Therefore, the ratio of average current to the number of Taylor cones decreases as a result of increasing concentration.

Figure 5.15 contains the graph that shows linear increase in diameters of nanofibers as the concentration of polyvinyl alcohol increases. As mentioned earlier, increasing concentration of polyvinyl alcohol increase the amount of solution brought on top of the spinning roller, hence the throughput per jet increases leading to large fiber diameter formation.

### 5.3.2 Effect of roller speed on roller electrospinning

This section contains the results of spinning one solution, 12%PVA, in different roller speed. The results are tabulated in tables and graphs. The conditions of electrospinning are tabulated in table 5.4.

**Table 5.4:** The table tabulates the parameters of electrospinning for the investigation of the effect of roller speed (rpm).

Roller-Collector Distance (mm)	Relative Humidity (%)	Temperature (C°)	Fabric collector speed (cm/min)	Applied Voltage (kV)	Roller Speed(rpm)	Polymer
120	30	23	10	55	1.5, 2, 3, 4,5	12%PVA

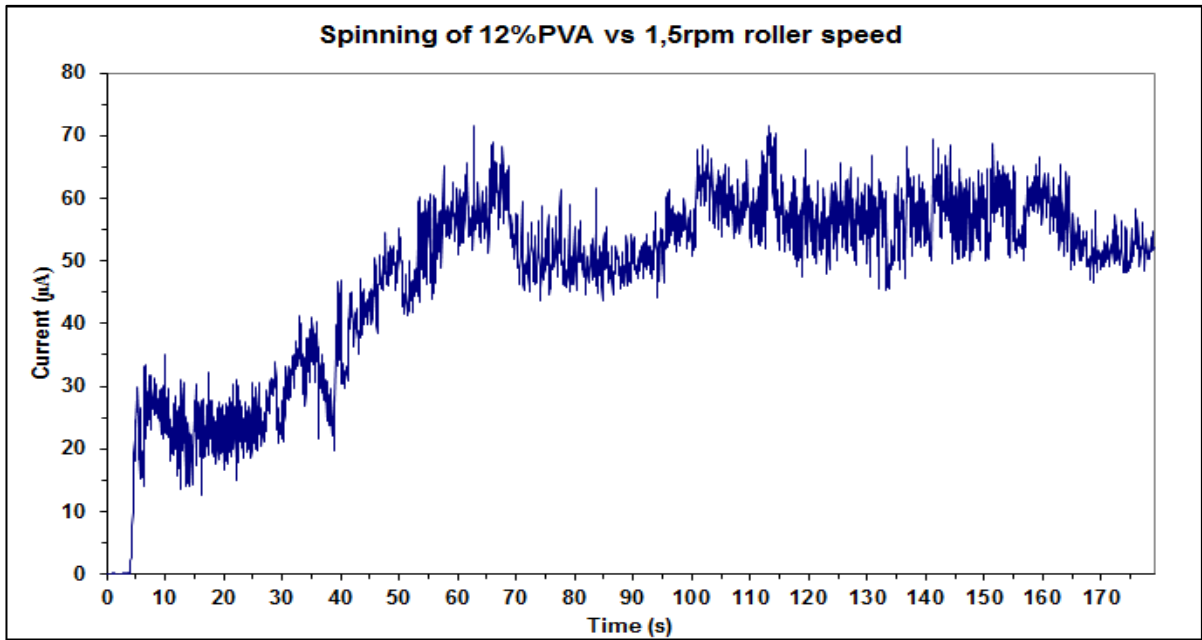


**Figure 5.17:** Graph of the current ( $\mu\text{A}$ ) flowing through the system in electrospinning of 12%PVA solution versus time (s) while roller speed was 1.5 rpm.

The graph in figure 5.15 shows the increase in current in first 60 seconds, and then the stable state is reached, where the flow of current is not changing.

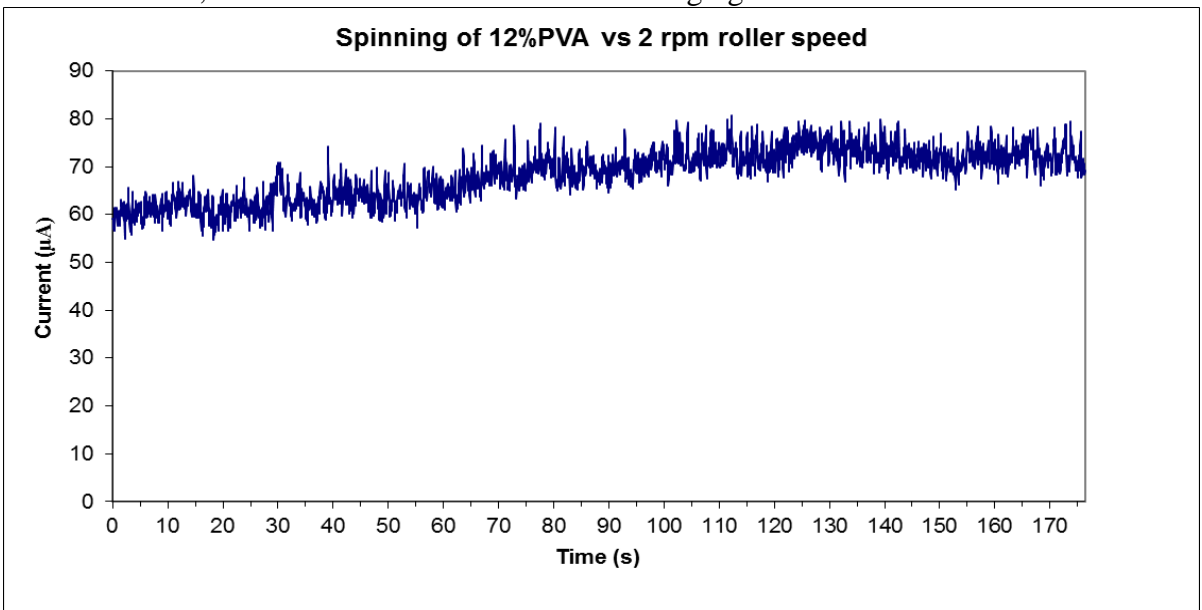


**Figure 5.18:** Graph of the current ( $\mu\text{A}$ ) flowing through the system in electrospinning of 12%PVA solution versus time (s).



There is slightly increase in current in the first 75- 80 seconds. After 80 seconds the current is constant. At time equal to zero second, the current is 60 $\mu$ A because of the continuity from roller speed of 1.5 rpm experiment, without switching off voltage but only changed the roller speed to 2 rpm.

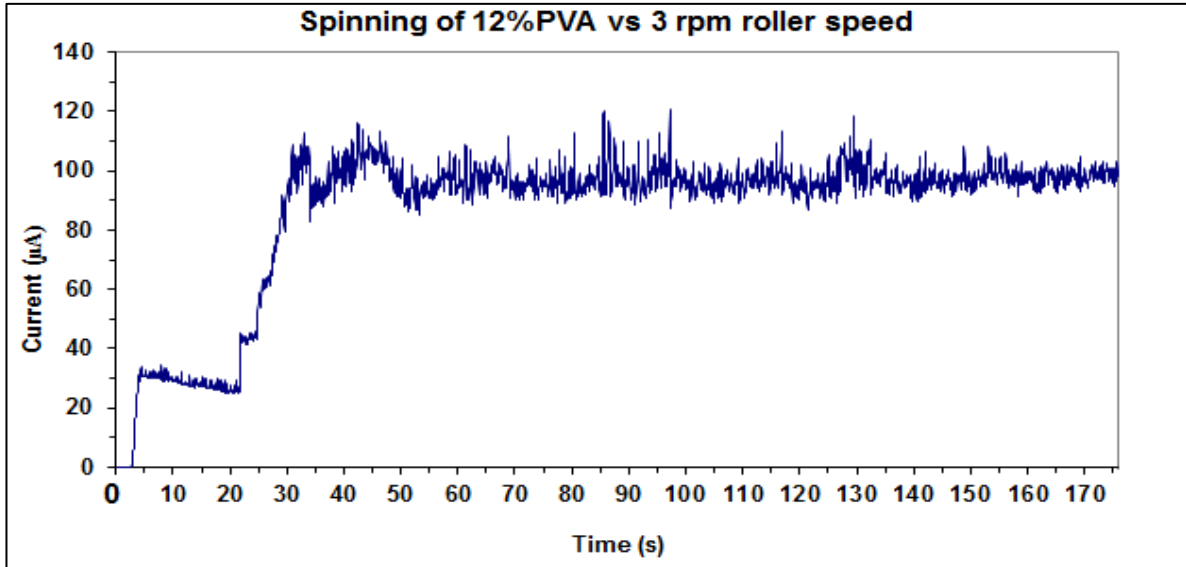


**Figure 5.19:** Graph of the current ( $\mu$ A) flowing through the system in electrospinning of 12%PVA solution versus time (s) while roller speed was 3 rpm.

The graph shows the increase in current for the first 30 seconds, reaching 100 $\mu$ A. After 30 seconds the current remains constant with 100 $\mu$ A.

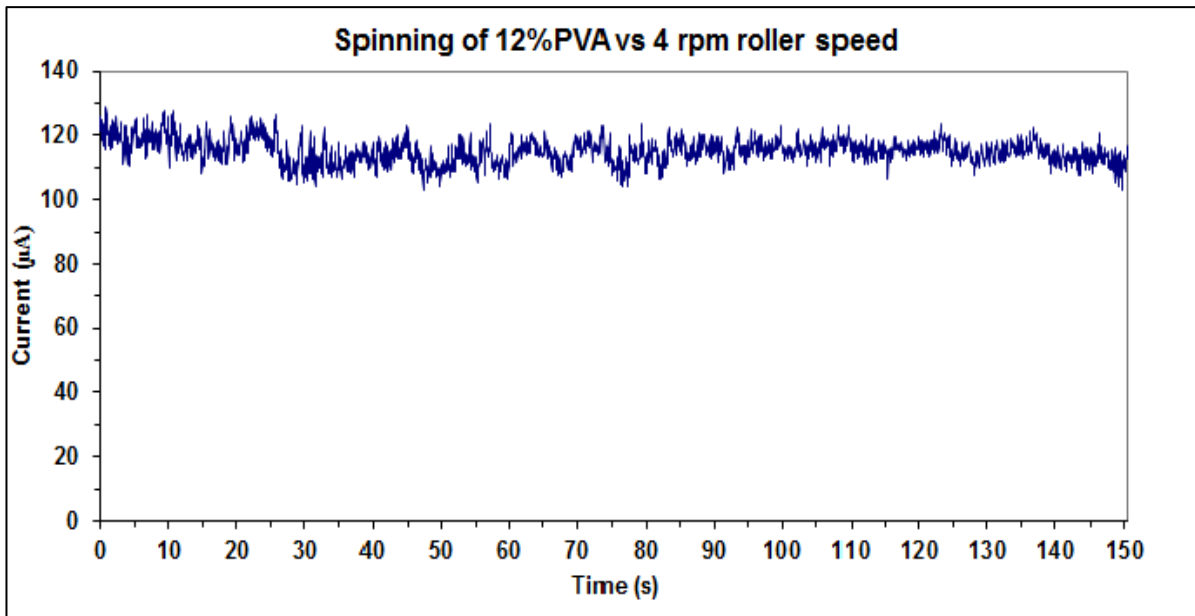


**Figure 5.20:** Graph of the current ( $\mu$ A) flowing through the system in electrospinning of 12%PVA solution versus time (s) while roller speed was 4 rpm.

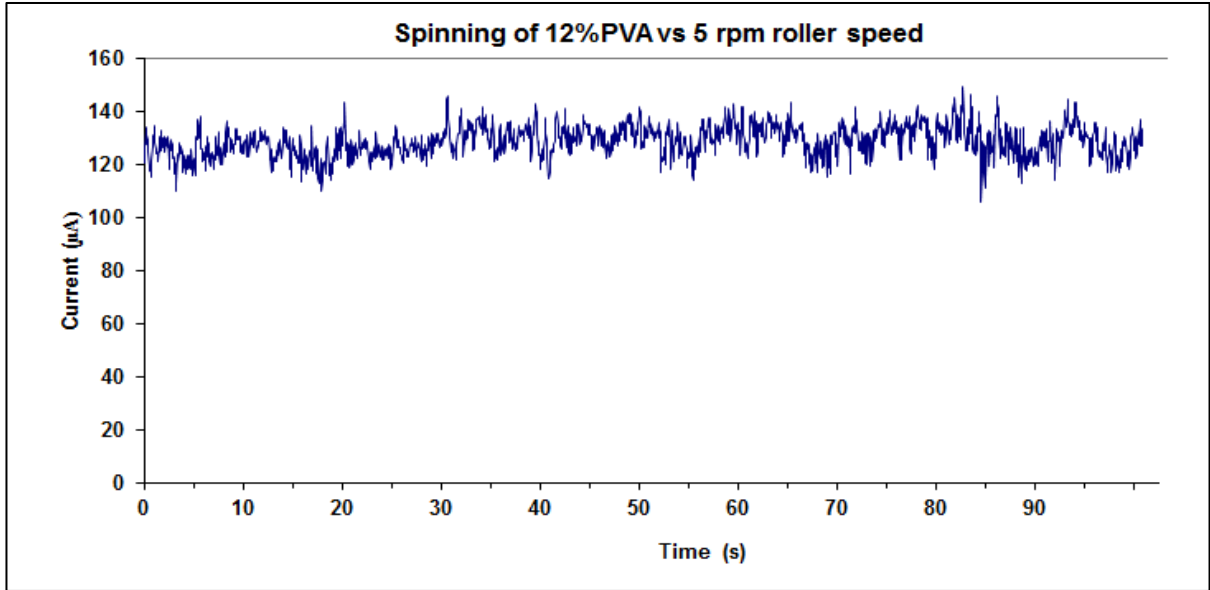


**Figure 5.21:** Graph of the current ( $\mu\text{A}$ ) flowing through the system in electrospinning of 12%PVA solution versus time (s) while roller speed was 5 rpm.

The table below, table 5.5, contains parameters of electrospinning due to changing the speed of electrospinning roller. Some of the parameters were mathematically extracted from the main parameters .i.e. throughput per jet, current per jet, etc, whereas others were visually observed durring experiment .e.g. number of Taylor cones. The graph of these parameters are plotted to futher analyze the relationship of these parameters with roller speed.

**Table 5.5:** The table contains parameters that depend on roller speed for electrospinning of 12%PVA solution.

Sample	Roller speed (rpm)	Avr. Current ( $\mu\text{A}$ )	Std.Dev ( $\mu\text{A}$ )	Fabric length (m)	Fabric Throughput (g/min/m)	number of Taylor cones	Throughput/jet (g/min)	Current/jet ( $\mu\text{A}$ )
12%PVA	1,5	47	14.7	0.24	0,6836	82	0,008	0,57
	2	68	5.2	0.245	0,7801	105	0,007	0,65
	3	97	4.6	0.26	1,2641	125	0,010	0,78
	4	115	3.8	0.25	1,2506	133	0,009	0,86
	5	129	5.8	0.255	1,625	140	0,012	0,92

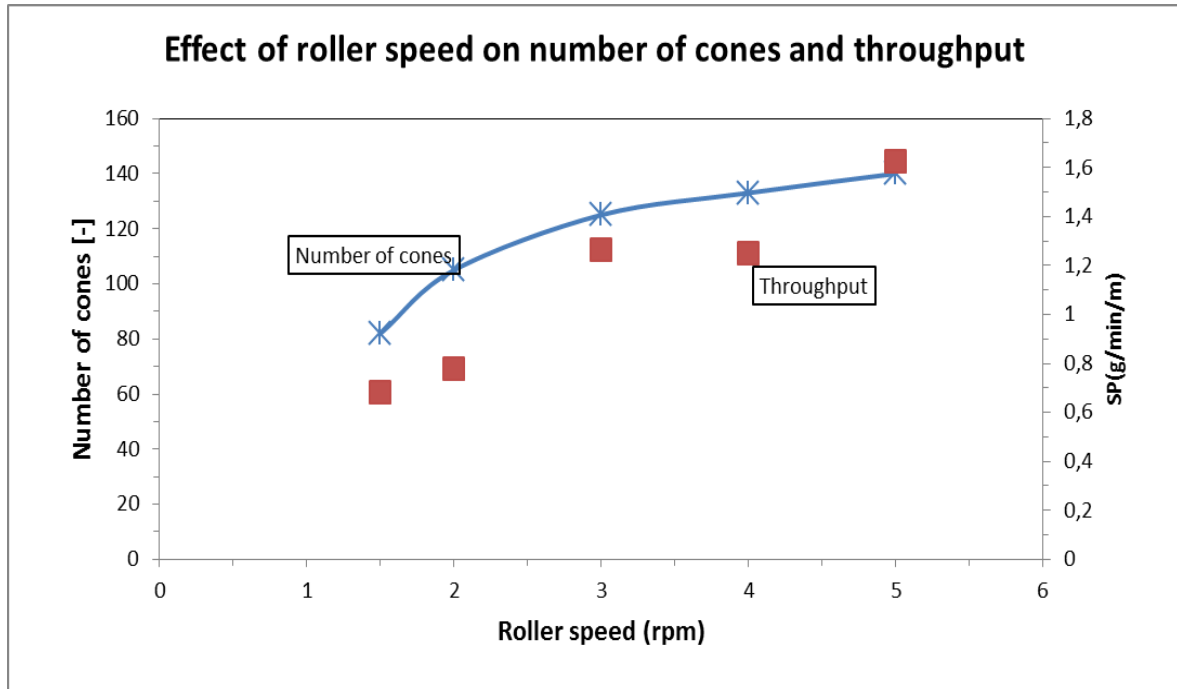


**Figure 5.22:** Graph of spinning performance or throughput SP (g/min/m) versus roller speed (rpm).

The graph in figure 5.21 shows that the increase in roller speed caused an increase in throughput of the nanomaterial. The relationship between the roller speed and spinning throughput is linearly dependence.

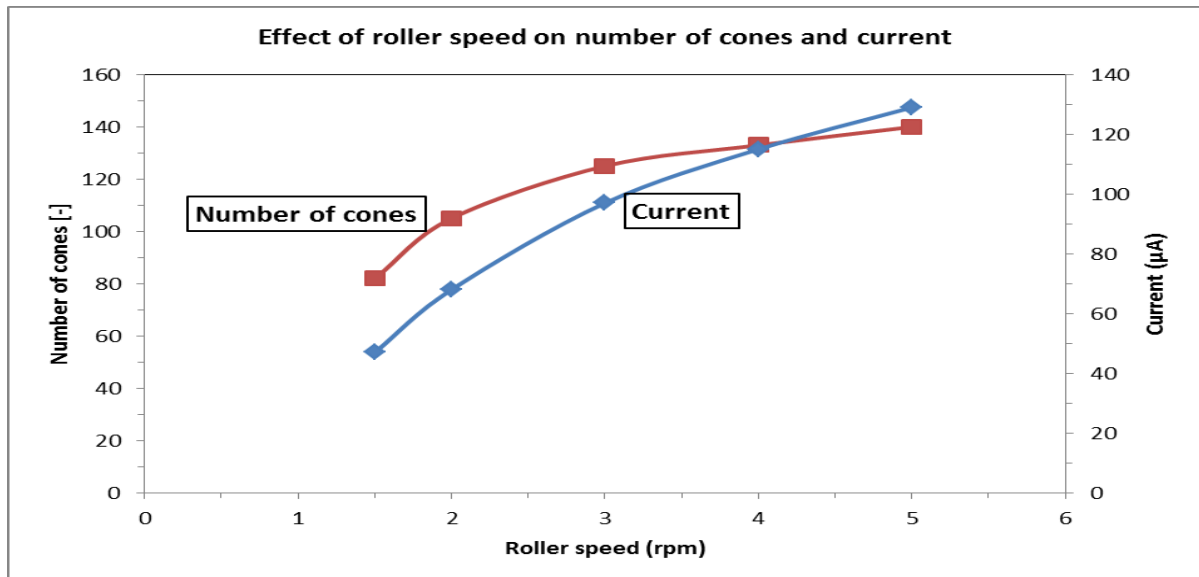


**Figure 5.23:** The graph shows the dependence of number of Taylor cones and electrical current on roller speed.

The graph indicates an increase in both the number of Taylor cones and electrical current due to the increase in roller speed. The relationship is considered to be power relation, with exponent greater than zero but less or equal to one.

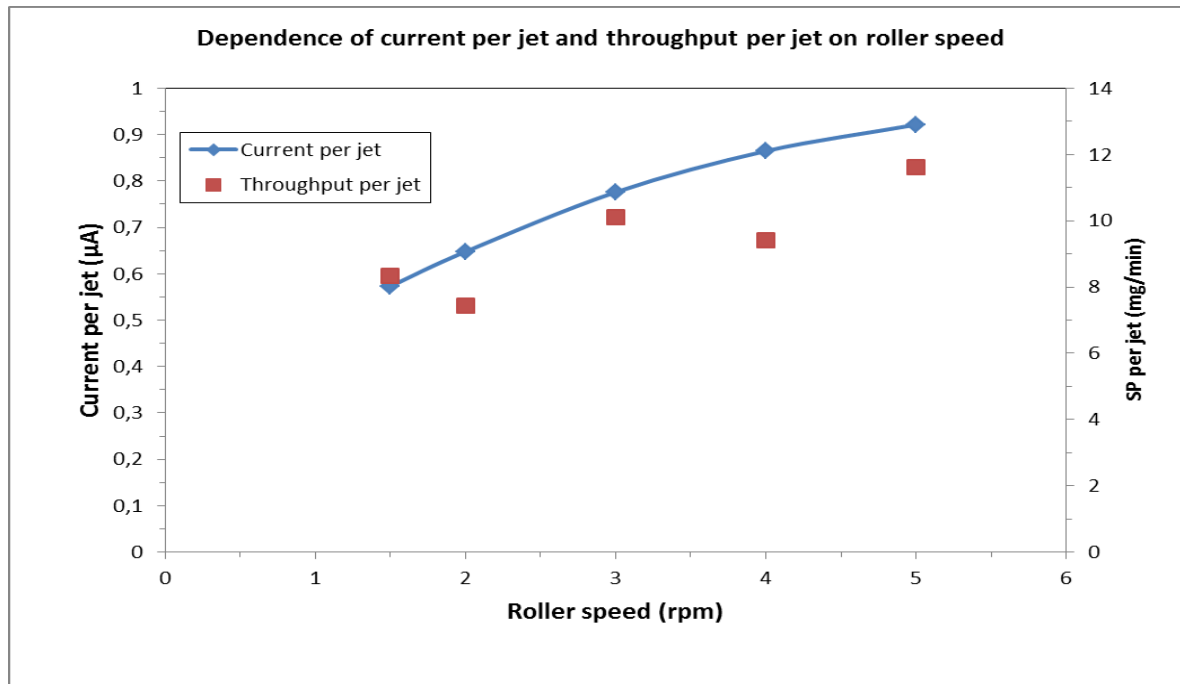


**Figure 5.24:** The graph shows the effect of roller speed on current per jet ( $\mu\text{A}$ ) and throughput per jet SP/jet ( $\text{g}/\text{min}$ ).

The current per jet shown in graph 5.3.2 increased with an increase in roller speed. The current per jet is clearly linear dependent to roller speed. The graph also indicates the increase in throughput per jet caused by an increase in roller speed.

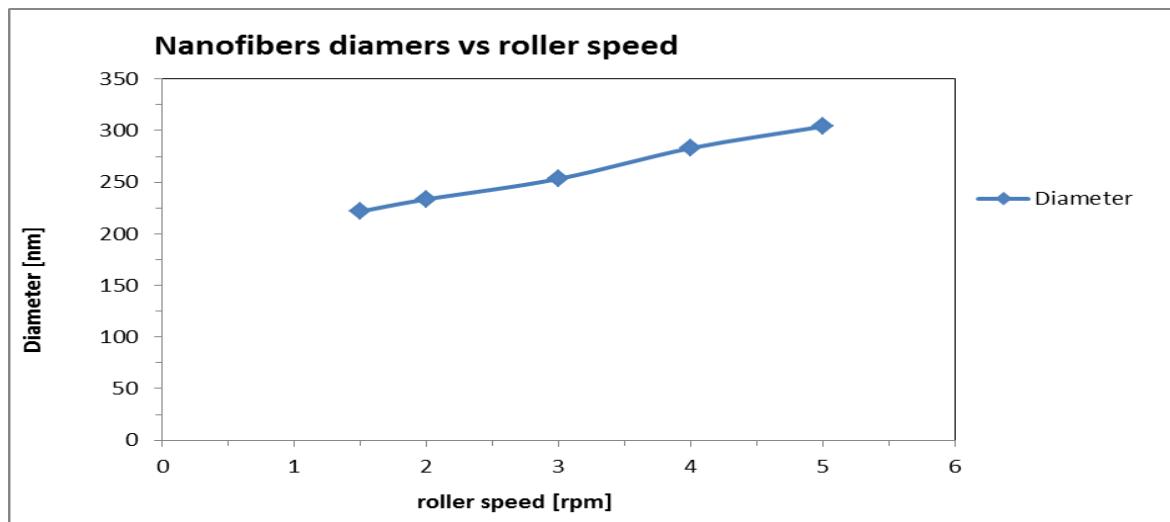


**Figure 5.25:** The graph of nanofibers diameters (nm) as a function of roller speed (rpm).

### Discussion of section 5.3.2

The current test used to analyze the process of electrospinning in terms of current conducted by polymer solution. As the roller speed is increased, the average current conducted by polymer solution also increases. The comparison of graphs of spinning by 1.5 rpm to 5 rpm shows high average current conducted for 5 rpm, and the minimum average current conducted during spinning with 1.5 rpm. When the roller rotates, it brings the polymer solution on top of itself .i.e. the polymer solution is positioned in a spin-able position; therefore if the roller speed is increased, more polymer solution is brought on the spin-able position in a short time interval. Then the number of cone increases. This phenomenon allows more polymers to be spun, conducting current between roller and collector increases. In spinning by slower rotating roller, it takes longer time for the system to reach the level of the average current; as the roller start rotating there is not enough polymer solution on top of the roller, but as it continue to rotate the thickness of the layer of the polymer solution on top of the roller increase until it reaches the state of equilibrium. Figure 5.21, 5.22 and 5.23 show a relations due to the increase in amount of polymer solution brought on top of the spinning roller as the its speed increases. The calculations and graphs of throughput in this work produced an unclear relations, this is due to the unevenness of the spinning .i.e. the higher throughput is obtained from the area that had high number of Taylor cones during spinning, and vice versa.

### 5.3.3 Effect of sodium salt on roller electrospinning

This section contains the results and discussion of the effect of sodium chloride salt on electrospinning. The results are tabulated in tables and shown in graphs for analysis. The results in this section are related to the effect of solution viscosity as a function of concentration on the roller movement. Therefore, sodium chloride was added to the 12 % PVA solution to investigate its (NaCl) effect on viscosity. And at the end the outcome of sodium chloride on spinning was tested. The roller speed was kept constant at 2.5 rpm.

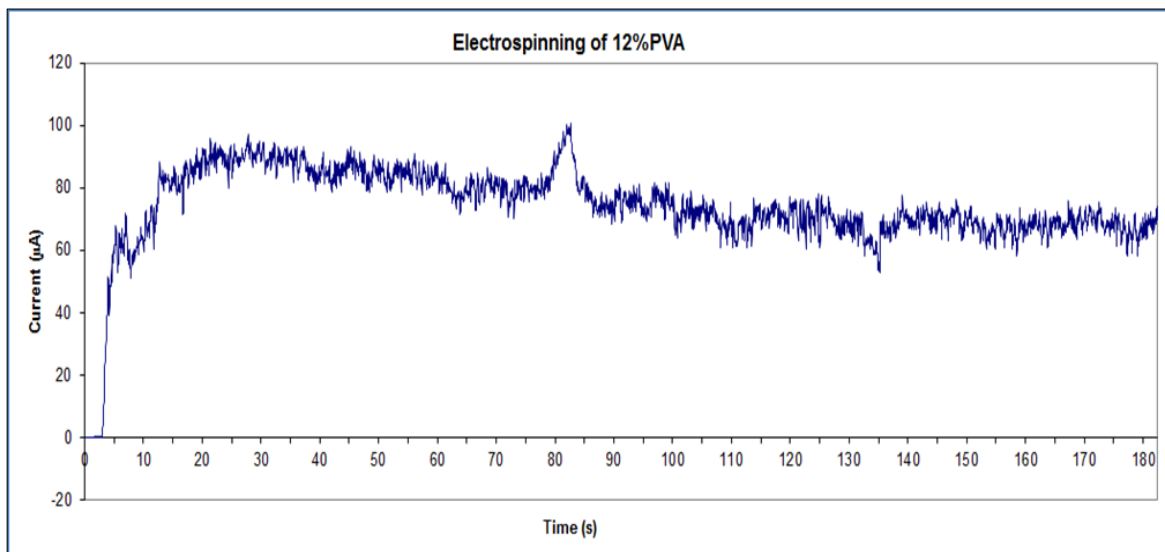


**Figure 5.26:** Graph of electrical current ( $\mu\text{A}$ ) in electrospinning of 12% PVA solution without NaCl versus time (s).

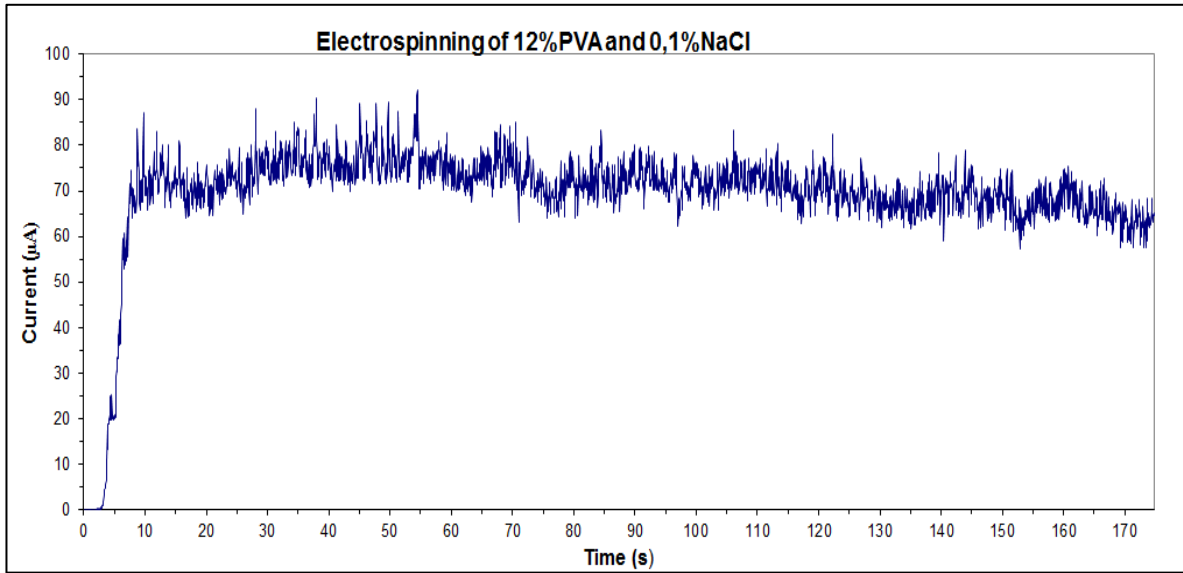


**Figure 5.27:** Graph of electrical current ( $\mu\text{A}$ ) flowing through the system during electrospinning of 12% PVA with 0.1%NaCl solution versus time (s).

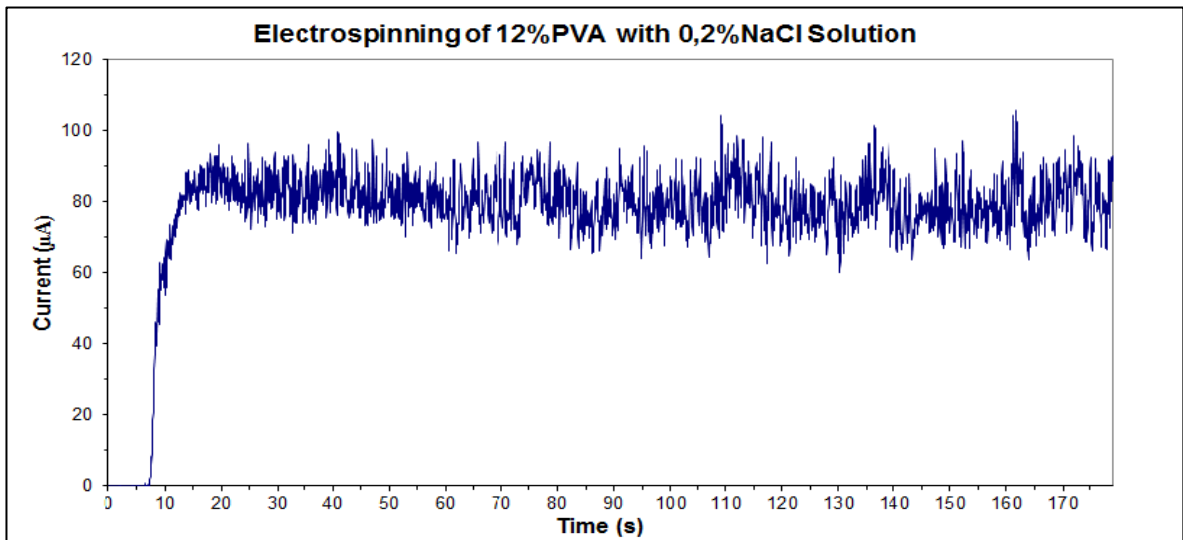


**Figure 5.28:** Graph of electrical current ( $\mu\text{A}$ ) flowing through the system during electrospinning of 12% PVA with 0.2%NaCl solution versus time (s).

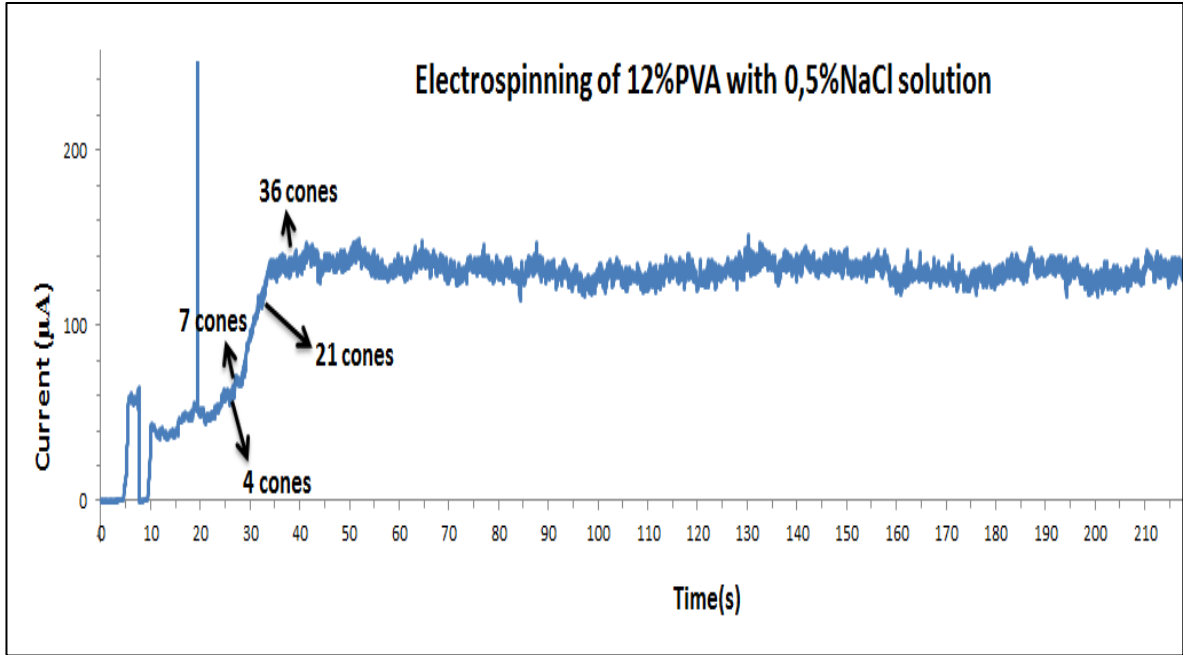


**Figure 5.29:** Graph of electrical current ( $\mu\text{A}$ ) flowing through the system during electrospinning of 12% PVA with 0.5%NaCl solution versus time (s).

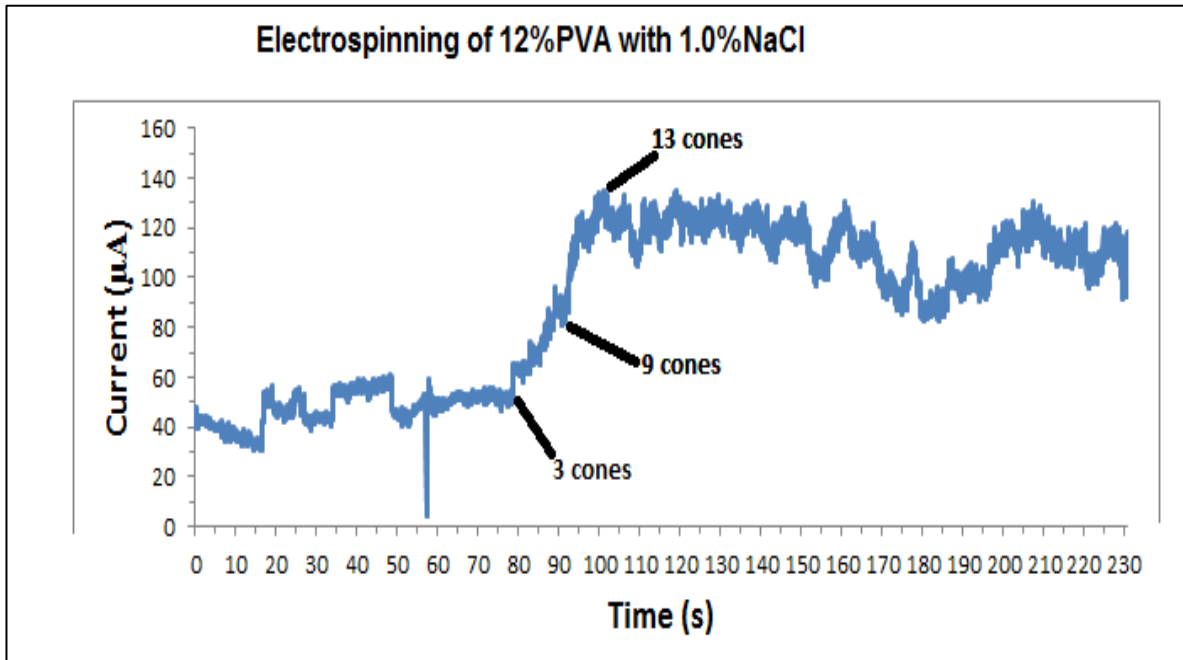


**Figure 5.30:** Graph of electrical current ( $\mu\text{A}$ ) flowing through the system during electrospinning of 12% PVA with 1%NaCl solution versus time (s).

**Table 5.6:** The table contains dependent parameters in different sodium chloride concentration.

sample	Avr. Current (μA)	Fabric Throughput (g/min/m)	number of Taylor cones	Throughput/jet (g/min)	Current/jet (μA)	Starting time of Taylor cone formation (s)
12%PVA	81,15	0,11	90	0.012	0.99	1,35
12%PVA+0.1% NaCl	81,81	0.64	72	0.009	0.97	8
12%PVA+0.2% NaCl	149,21	0.62	70	0.009	1.94	16,7
12%PVA+0.5% NaCl	131,92	0.49	45	0.011	2.78	22
12%PVA+1.0% NaCl	112,37	0.13	16	0.008	7.54	61,95

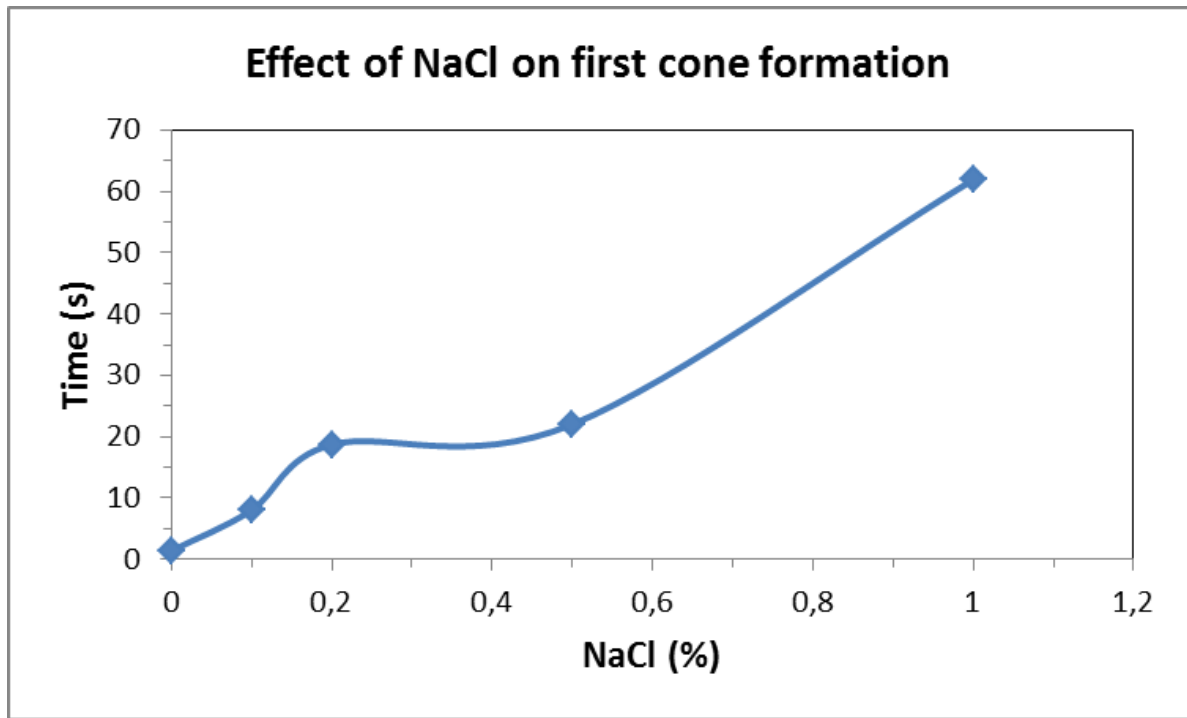


**Figure 5.31:** Graph shows the starting time (s) of cone formation versus sodium chloride, NaCl concentration (%).



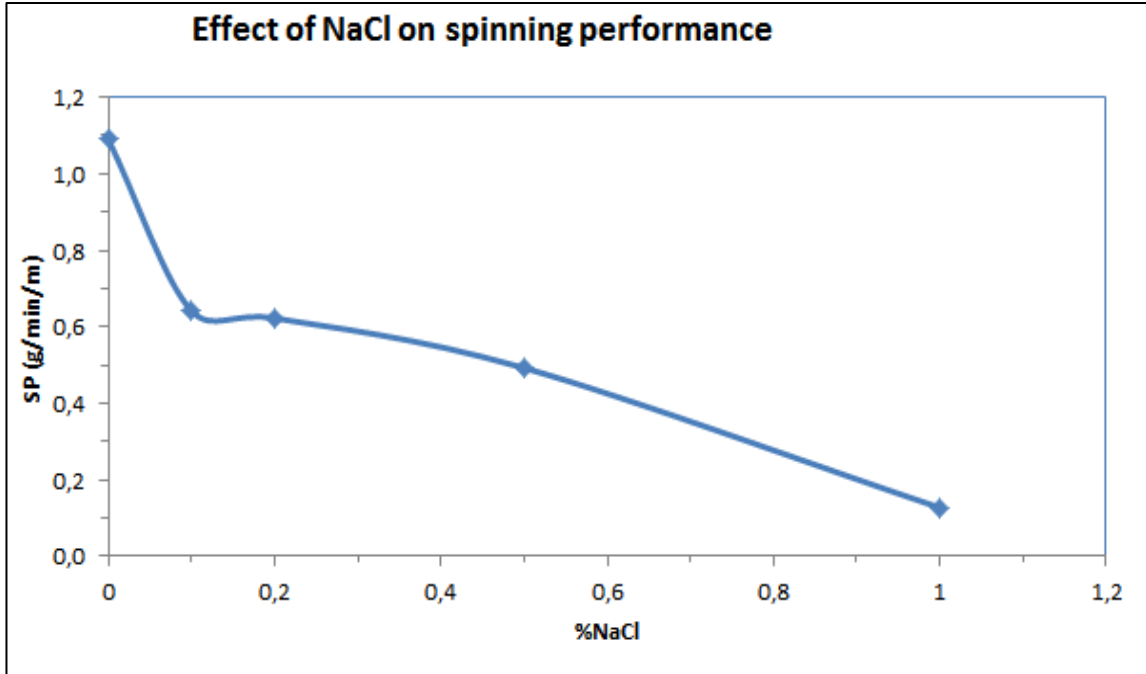


**Figure 5.32:** Graph of spinning performance SP (g/min/m) versus sodium chloride NaCl concentration (%).

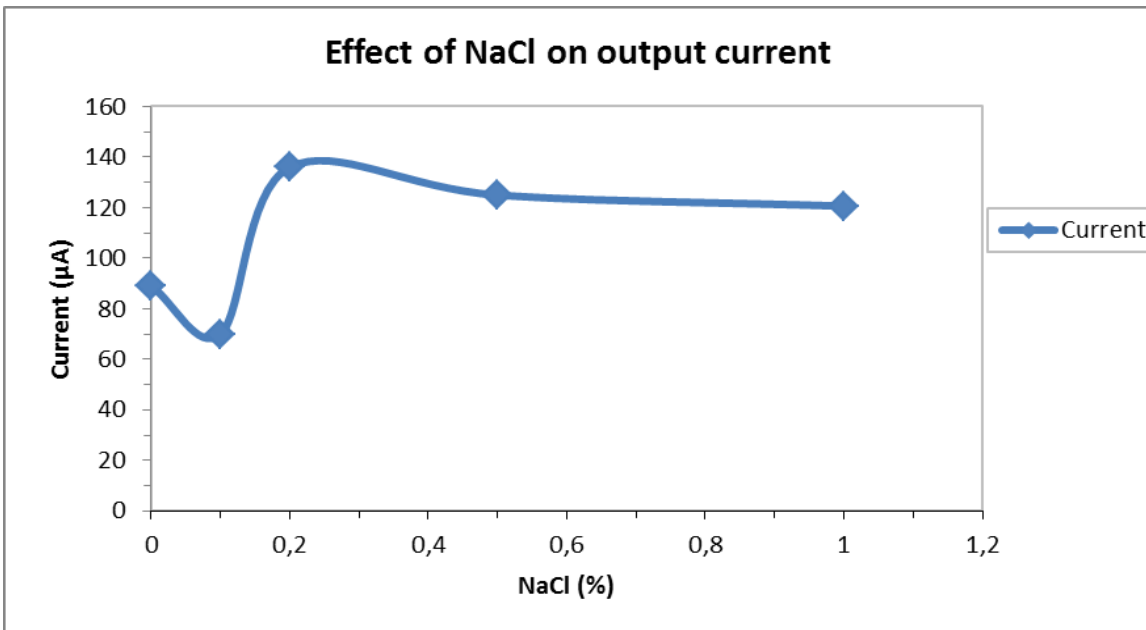


**Figure 5.33:** Graph of current (µA) flowing through the spinning system versus sodium chloride concentration (%) in a polyvinyl alcohol solution.

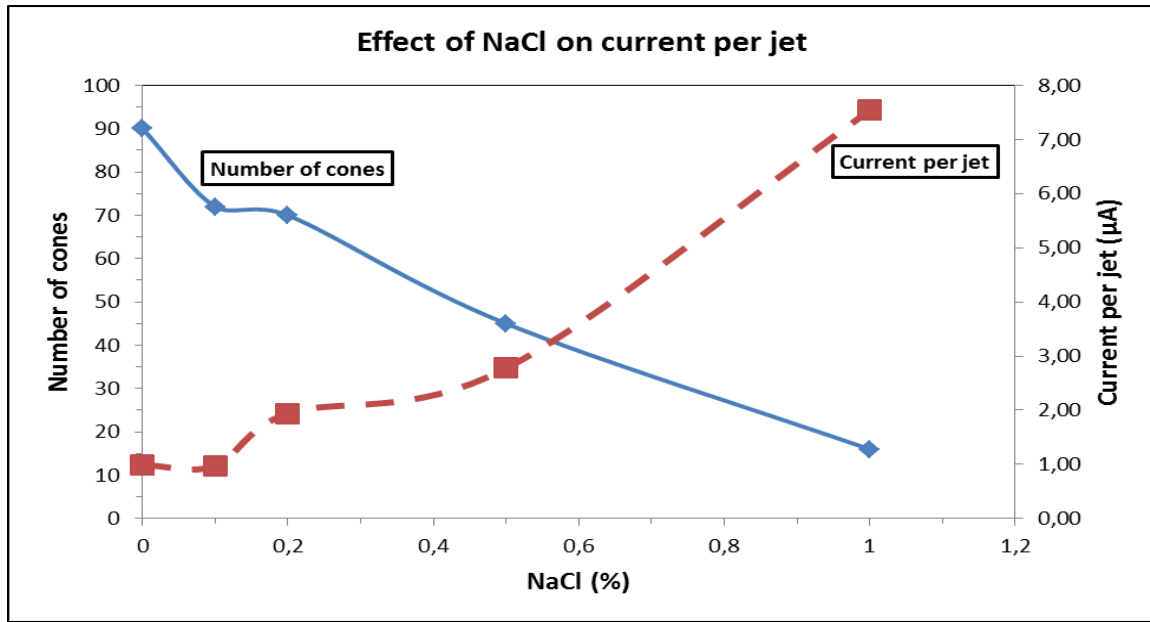


**Figure 5.34:** Graph shows the dependence of number of Taylor cones and current per jet on sodium chloride concentration.

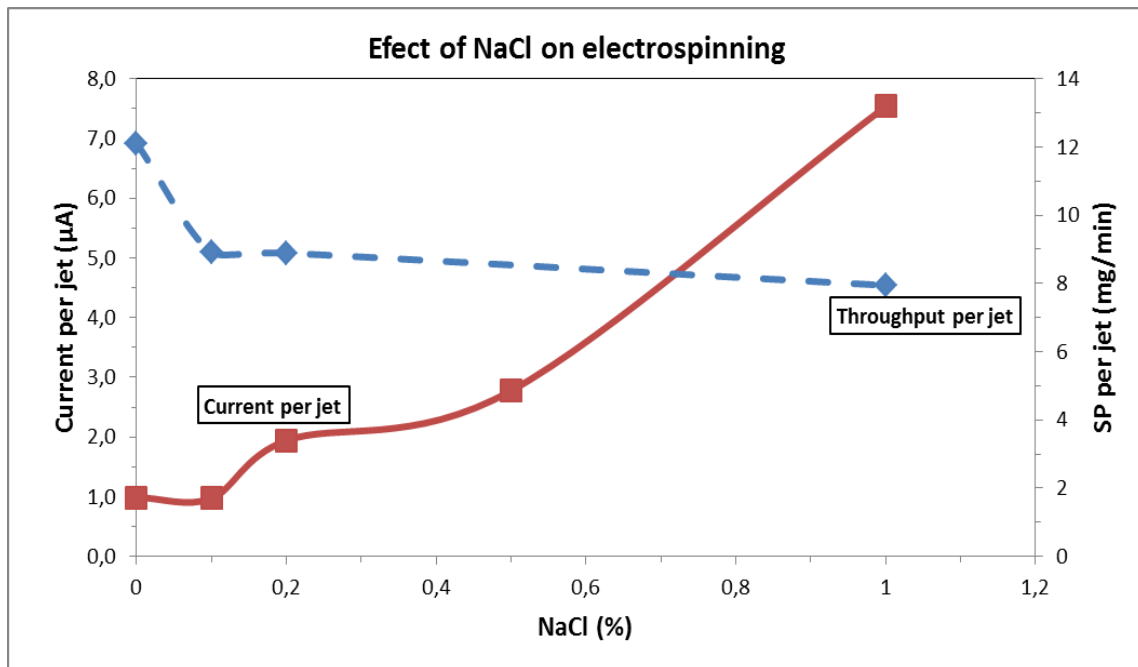


**Figure 5.35:** Graph shows the dependence of spinning performance per jet (mg/min) and current (µA) per jet on sodium chloride concentration.

Figure 5.35 contains the graph which shows that throughput per jet is inversely proportional to concentration of sodium chloride in polyvinyl alcohol solution. The graph also indicates that current per jet increases as the sodium chloride content increases in PVA solution.

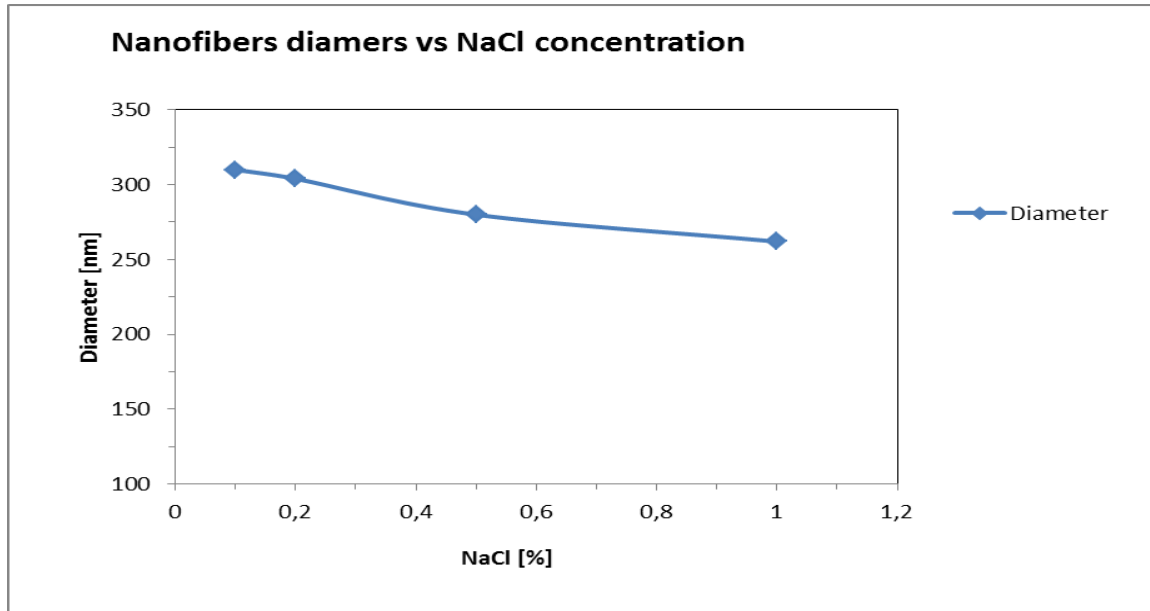


**Figure 5.36:** Graph of fiber diameters (nm) as function of concentration (%) of sodium chloride in polyvinyl alcohol solution.

The graph above shows that diameter of the nanofibers is inversely proportional to the concentration of sodium chloride in polyvinyl alcohol solution.

### Discussion of section 5.3.3

Table 5.6 shows that the starting time for the first cone to appear onto the spinning roller is increasing with an increase in sodium chloride content in a solution. The addition of salt increases the density of ions in the polymer solution, and then electrical potential increases simultaneously causing the instability in the solution, delaying the formation of Taylor cones.

Owing to the instability of polymer solution, the number of Taylor cones decreases with an increase in sodium chloride salt. Fewer Taylor cones formed resulted in low throughput and then low average current .i.e. the addition of salt decreased the number of Taylor cones formed, causing fewer fibers to be spun, this is valid if amount of polymer solution contained in each cone is not increasing.

Even though the amount of polymer solution transferred was decreasing with an increase in salt content, the current per jet flowed between spinning roller and collector increased; this is due to the fact that sodium chloride increases the density of ions in a solution causing an increase in conductivity, therefore, the current per jet increases.

## Chapter 6 : Conclusion

This study has improved and simplified the technology of electrospinning .i.e. One more parameter added to this technology of spinning nanofibers by roller expands the options of controlling the spinning process as well as the morphology of the produced material. This work showed that thickness of the layer of the polymer solution onto the spinning roller is important during the process of spinning, also important for the properties of nanomaterial produced and nanofibers themselves.

During this study was found that thickness of the layer of the polyvinyl alcohol solution is increasing when the angular speed of spinning roller is increasing. The thickness of the layer of the PVA solution is directly proportional to the concentration of the polyvinyl alcohol in the spinning solution. During the study, it was witnessed that the thickness of the layer is more linearly dependent on the viscosity of the polymer solution.

However, these experimental results differ from what is stated by the theories; equation 2.1 and 2.2 both state that the thickness of the layer is dependent on the square root of the viscosity, but mathematical solutions from the theory allows the conclusion of thickness of the layer to be proportional to the square root of solution viscoscity. Nevertheless, the results and theory in chapter 2 agree on the increase of thickness regarding the increase in viscosity.

This work provided the evidence that the thickness of the layer of the PVA solution has the positive influence on the number of cones on the spinning roller and amount of polymer solution contained in each polymer jet (throughput per jet). Concurrently, the throughput of the material is high with the large diameters of nanofibers.

It can be concluded that using sodium chloride to change the viscosity of the polyvinyl alcohol causes a series of downfall, from spinning process up to the properties of the nanofibrous material and to nanofibers themselves. Adding sodium chloride into the spinning PVA solution delays the starting time of the formation of cones, it lowers the throughput per jet during electrospinning. The throughput of the material and diameters of nanofibers decreases with an increase of sodium chloride.

The drawn conclusion shows that roller movement in roller electrospinning is the one of the most important parameters in this technology of producing nanofibers.

## References

- [1] Frenot A, Chronakis I.S; Polymer nanofibers assemble by electrospinning; IFP Research, Swedish Institute for Fiber and Polymer Research.
- [2] Jirsak O, Petrik S; Needleless Electrospinning –History, Present and Future; 2010.
- [3] Ing. DAO T.A; The Role Of Rheological Properties Of Polymer Solutions In Needleless Electrostatic Spinning;2010.
- [4] Ramakrishna.S, Fujihara. K, Teo. W, Lim. T, and Ma. Z, An introduction to electro spinning and nanofibres, World Scientific Publishing Co., Singapor, 2005.
- [5] Dosh J, Reneker DH, Electrospinning process and applications of electrospun fibers, by J Electrostatics 1995.
- [6] Deitzel J M, Kleimeyer J; Harris D, Tan NCB, Effect of processing variables on the morphology of electrospun nanofibers and Textiles, Polymer 42 No 1, 2001, p.261.
- [7] Haghi AK, Akbari M. Trends in electrospinning of natural nanofibers. Phys Status Solidi2007;204: 1830-4.
- [8] Ki CS, Baek DH, Gang KD, Lee KH, Urn IC, Park YH. Characterization of gelatin nanofiber prepared from gelatin-formic acid solution. Polymer 2005;46:5094-102.
- [9] M.M. Hohman, M. Shin and G. Rutledge, Electrospinning and electrically forced jets,I, Stability theory, Physics of Fluids, 2001, 13, 8, 220 l.
- [10] Pham QP, Sharma U, Mikos AG. Electrospun poly (s-caprolactone) micro fiber and multilayer nanofiber/microfiber scaffolds: characterization of scaffolds and measurement of cellular infiltration. Biomacromolecules 2006;7:2796-805.
- [11] Deitzel J M; Kleimeyer J; Harris D; Tan NCB, Effect of processing variables on the morphology of electrospun nanofibers and Textiles, Polymer 42 No 1, 2001, p.261.
- [12] Haghi AK, Akbari M. Trends in electrospinning of natural nanofibers. Phys Status Solidi 2007;204: 1830-4.
- [13] Brown P.J and Stevens K, Nanofibers and nanotechnology in textiles, Woodhead Publishing Limited and CRC Press LLC, 2007.
- [14] Mckee MG, Wilkes GL, Colby RH, Long TE. Correlations of solution rheology with electrospun fiber formation of linear and branched polyesters. Macromolecules 2004;37: 1760-7.
- [15] McKee, M. G., T. Park, S. Unal, I. Yilgor, and T. E. Long (2005). "Electro spinning of linear and highly branched segmented poly(urethane urea)s." Polymer 46(7):2011-2015.
- [16] Shenoy S L; Bates W D; Frisch H L; Wnek G E, Role of chain entanglements on fiber formation during electrospinning of polymer solutions: good solvent, non-specific polymerpolymer interaction limit, Polymer 46 (2005) 3372-3384.

- [17] Hayati I, Bailey AI, Tadros TF. Investigations into the mechanisms of electrohydrodynamic spraying of liquids. 1. Effect of electric-field and the environment on pendant drops and factors affecting the formation of stable jets and atomization. *J Colloid Interface Sci* 1987; 117:205-21.
- [18] Kim B, Park H, Lee SH, Sigmund WM. Poly (acrylic acid) nanofibers by electrospinning. *Mater Lett* 2005;59:829-32.
- [19] A.T. DAO and O. Jirsak, Effect of Sodium Chloride on the needle electro spinning of poly (vinyl alcohol), Nanocon 2009 - 1<sup>st</sup> Conference with International Participation, Roznov, Czech Republic, ED ZO<sup>''</sup> - 22<sup>nd</sup> October 2009.
- [20] Huang L, Nagapudi K, Apkarian RP, Chaikof EL. Engineered collagen-PEO nanofibers and fabrics. *J Biomater Sci Polym Ed* 2001 ;12:979-93
- [21] Jiang HL, Fang DF, HsiaoBS, Chu B, Chen WL. Optimization and characterization of dextran membranes prepared by electrospinning. *Biomacromolecules* 2004a;5: 326-33.
- [22] Mit-uppatham C, Nithitanakul M, Supaphol P. Ultrafine electrospun polyamide-6 fibers: effect of solution conditions on morphology and average fiber diameter. *Macromol Chern Physics* 2004; 205:2327-38.
- [23] Krishnappa, R. V. N., Sung, C. M. and Schreuder-Gibson, H. (2002). Electrospinning of Polycarbonates and their Surface Characterization using the SEM and TEM. *Mat. Res. Soc. Symp. Proc.* 702, pp. U6.7.1-6.7.6.
- [24] Larrondo L, Manley RSJ. Electrostatic fiber spinning from polymer melts. 1. Experimental observations on fiber formation and properties. *J Polym Sci, Polym Phys Ed* 1981a; 19:909-20.
- [25] Larrondo L, Manley RSJ. Electrostatic fiber spinning from polymer melts. III. Electrostatic deformation of a pendant drop of polymer melts. *J Polym Sci, Polym Phys Ed* 1981; 19:933-40.
- [27] Yordem OS, Papila M, Menciloglu YZ. Effects of electrospinning parameters on polyacrylonitrile nanofiber diameter: an investigation by response surface methodology. *Mater Des* 2008; 29:34-44.
- [28] Wang X, Urn IC, Fang D, Okamoto A, Hsiao BS, Chu B. Formation of water-resistant hyaluronic acid nanofibers by blowing-assisted electro-spinning and non-toxic post treatments. *Polymer* 2005; 46:4853-67.
- [29] Sundaray B, Subramanian V, Natarajan TS, Xiang RZ, Chang CC, Fann WS. Electrospinning of continuous aligned polymer fibers. *Appl Phys Lett* 2004; 84: 1222--4.
- [30] Li D, Wang Y, Xia Y. Electrospinning nanofibers as uniaxially aligned arrays and layer-by-layer stacked films. *Adv Mater* 2004; 16:361-6.

- [31] Xu CY, Inai R, Kotaki M, Ramakrishna S. Aligned biodegradable nanofibrous structure: a potential scaffold for blood vessel engineering. *Biomaterials* 2004; 25:877-86.
- [32] Ki CS, Kim JW, Hyun JH, Lee KH, Hattori M, Rah DK, et al. Electrospun three dimensional silk fibroin nanofibrous scaffold. *J Appl Polym Sci* 2007; 106:3922-8.
- [33] Kumbar SG, Nukavarapu SP, James R, Hogan MV, Laurencin CT. Recent patents on electrospun biomedical nanostructures: an overview. *Biomed Eng* 2008; 1:68-78.
- [34] Reneker DH, Varin AL, Fong H, Koombhongse S. Bending instability of electrically charged liquid jets of polymer solutions in electrospinning. *J Appl Phys* 2000;87:4531-47.
- [35] Shin YM, Hohman MM, Brenner MP, Rutledge Gc. Experimental characterization of electrospinning: the electrically forcedjet and instabilities. *Polymer* 2001.
- [36] Doshi J, Reneker DH. Electrospinning process and applications of electro spun fibers. *J Electrostat*;1995.
- [37] Fong H, Liu WD, Wang CS, Vaia RA. Generation of electro spun fibers of nylon 6 and nylon 6-montmorillonite nanocomposite. *Polymer* 2002; 43:775-80.
- [38] Li D, Wang Y, Xia Y. Electrospinning of polymeric and ceramic nanofibers as uniaxially aligned arrays. *Nano Lett* 2003.
- [39] Jalilt R, Morshed M, Abdolkarim S, Ravandi H. Fundamental parameters affecting electrospinning of PAN nanofibers as uniaxially aligned fibers. *J Appl Polym Sci* 2006.
- [40] Deitzel J M, Kleimeyer J, Harris D, Tan NCB; Effect of processing variables on the morphology of electrospun nanofibers and Textiles, *Polymer* 42 No 1; 2001.
- [41] Koski, A., K. Vim, and S. Shivkumar (2004). "Effect of molecular weight on fibrous PVA produced by electrospinning." *Materials Letters* 58(3-4):493-497.
- [42] Casper, C. L., W. Yang, M. C. Farach-Carson, and I. F. Rabolt (2006). "Understanding the effects of processing parameters on electro spun fibers and applications in tissue engineering." In: *Polymeric Nanofibers*. ACS Symposium Series 918. Edited by D. H. Reneker and H. Fong. Oxford University Press (USA), p. 205.
- [43] Geng X, Kwon OH, Jang J. Electrospinning of chitosan dissolved in concentrated acetic acid solution. *Biomaterials* 2005;26:5427-32.
- [44] Zhao ZZ, Li JQ, Yuan XV, Li X, Zhang YY, Sheng I. Preparation and properties of electro spun poly (vinylidene fluoride) membranes. *J Appl Polym Sci* 2005;97: 466-74.

- [45] Casper CL, Stephens JS, Tassi NG, Chase DB, Rabolt JF. Controlling surface morphology of electrospun polystyrene fibers: effect of humidity and molecular weight in the electro spinning process. *Macromolecules* 2004;37:573-8.
- [46] Li M, Mondrinos MJ, Gandhi MR, Ko FK, Weiss AS, Lelkes PI. Electrospun protein fibers as matrices for tissue engineering. *Biomaterials* 2005;26:5999-6008.
- [47] K1 CS, Baek DH, Gang KD, Lee KH, Um IC, Park YH. Characterization of gelatin nanofiber prepared from gelatin-formic acid solution. *Polymer* 2005;46:5094-102.
- [48] Lee JS, Choi KH, Ghim HD, Kim SS, Chun DH, Kim HY, et al. Role of molecular weight of a tactic poly (vinyl alcohol) (PV A) in the structure and properties of PV A nanofabric prepared by electrospinning. *J Appl Polym Sci* 2004;93:1638-46.
- [49] Pham QP, Sharma U, Mikos AG. Electrospun poly (s-caprolactone) micro fiber and multilayer nanofiber/microfiber scaffolds: characterization of scaffolds and measurement of cellular infiltration. *Biomacromolecules* 2006;7:2796-805.
- [50] Baumgarten PK. Electrostatic spinning of acrylic microfibers. *J Colloid Interface Sci* 1971;36:71-9.
- [51] Mit-uppatham C, Nithitanakul M, Supaphol P. Ultrafine electrospun polyamide-6 fibers: effect of solution conditions on morphology and average fiber diameter. *Macromol Chern Phys* 2004;205:2327-38.
- [52] Zhang C, Yuan X, Wu L, Han Y, Sheng J. Study on morphology of electrospun poly (vinylalcohol) mats. *Eur Polym J* 2005;41 :423-32.
- [53] Buchko CJ, Chen LC, Shen Y, Martin DC. Processing and microstructural characterization of porous biocompatible protein polymer thin films. *Polymer* 1999;40: 7397-407.
- [54] Li D, Wang Y, Xia Y. Electrospinning nanofibers as uniaxially aligned arrays and layer-by-layer stacked films. *Adv Mater* 2004; 16:361-6.
- [55] Campanella O.H, Cerro R.L, Viscous flow on the outside of a horizontal rotating cylinder, *Chemical Engineering Science*, 1984.
- [56] Benjamin D.F, Anderson T.J and Scriven L.E, Multiple roller systems: steady state operation.
- [57] Cerro R.L and Scriven L.E, Rapid free surface film flows. An integral approach *Industrial and Engineering Chemistry, Fundamentals*, 19 (1980), pp. 40-50
- [58] Cengiz F, Dao TA, Jirsak O; Influence of Solution Properties on the Roller Electrospinning of Poly (vinyl alcohol); Suleyman Demirel University, Technical University of Liberec; 2010.